

Enhanced Cardiac Differentiation of Human Cardiovascular Disease Patient-Specific Induced Pluripotent Stem Cells by Applying Unidirectional Electrical Pulses Using Aligned Electroactive Nanofibrous Scaffolds

Leila Mohammadi Amirabad,^{†,‡,§,¶} Mohammad Massumi,^{*,§,⊥} Mehdi Shamsara,^{*,†} Iman Shabani,[¶] Afshin Amari,[#] Majid Mossahebi Mohammadi,^{||} Simzar Hosseinzadeh,[‡] Saeid Vakilian,^{||} Sarah K. Steinbach,[□] Mohammad R. Khorramizadeh,[▲] Masoud Soleimani,^{||} and Jalal Barzin^{○,¶}

[†]Stem Cells Department, National Institute of Genetic Engineering and Biotechnology, Tehran, Iran

[‡]School of Advanced Technologies in Medicine, Shahid Beheshti University of Medical Sciences, Tehran, Iran

[§]Lunenfeld-Tanenbaum Research Institute, Mount Sinai Hospital, Toronto, Ontario M5T 3H7, Canada

[⊥]Department of Physiology, University of Toronto, Toronto, Ontario M5S 1A8, Canada

[¶]Biomedical Engineering Department, Amirkabir University of Technology, Tehran, Iran

[#]Cellular and Molecular Research Center, Ahvaz Jundishapur University of Medical Sciences, Ahvaz 61357-15794, Iran

^{||}Stem Cells Biology Department, Stem Cell Technology Research Center, Tehran, Iran

[□]McEwen Centre for Regenerative Medicine, Toronto, Ontario MSG 1L7, Canada

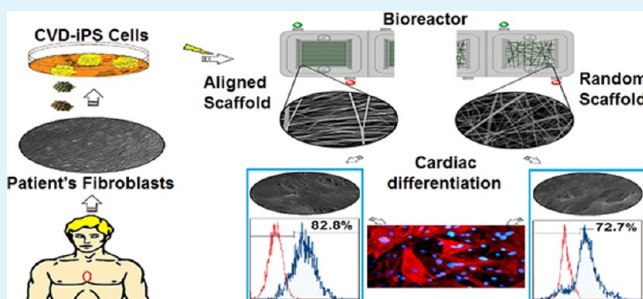
[▲]Endocrinology and Metabolism Molecular-Cellular Sciences Institute, Tehran University of Medical Sciences, Tehran, Iran

[○]Biomaterials Department, Iran Polymer and Petrochemical Institute, Tehran, Iran

Supporting Information

ABSTRACT: In the embryonic heart, electrical impulses propagate in a unidirectional manner from the sinus venosus and appear to be involved in cardiogenesis. In this work, aligned and random polyaniline/polyethersulfone (PANI/PES) nanofibrous scaffolds doped by Camphor-10-sulfonic acid (β) (CPSA) were fabricated via electrospinning and used to conduct electrical impulses in a unidirectional and multidirectional fashion, respectively. A bioreactor was subsequently engineered to apply electrical impulses to cells cultured on PANI/PES scaffolds. We established cardiovascular disease-specific induced pluripotent stem cells (CVD-iPSCs) from the fibroblasts of patients undergoing cardiothoracic surgeries. The CVD-iPSCs were seeded onto the scaffolds, cultured in cardiomyocyte-inducing factors, and exposed to electrical impulses for 1 h/day, over a 15-day time period in the bioreactor. The application of the unidirectional electrical stimulation to the cells significantly increased the number of cardiac Troponin T (cTnT+) cells in comparison to multidirectional electrical stimulation using random fibrous scaffolds. This was confirmed by real-time polymerase chain reaction for cardiac-related transcription factors (NKX2.5, GATA4, and NPPA) and a cardiac-specific structural gene (TNNT2). Here we report for the first time that applying electrical pulses in a unidirectional manner mimicking the unidirectional wave of electrical stimulation in the heart, could increase the derivation of cardiomyocytes from CVD-iPSCs.

KEYWORDS: *electrical impulse, cardiogenesis, PANI/PES fibrous scaffolds, iPSCs, cardiomyocytes*



1. INTRODUCTION

Cardiovascular diseases (CVDs) remain the leading cause of death in the world.¹ Because of the limited regeneration of adult cardiomyocytes, designing a functional engineered tissue using stem cells could be a promising approach to restore cardiac function after myocardial infarction or in severe heart failure. There are many unknown chemical and physical factors that can affect the generation of cardiomyocytes from stem cells.² One way to improve the

efficiency of cardiomyocyte cell generation is to recapitulate in vivo niche of cardiomyocytes in an in vitro cell culture system.

Unlike embryonic stem (ES) cells, induced pluripotent stem cells (iPSCs) can be derived from the affected patient cells and used for autologous cell therapy and drug screening. In contrast

Received: December 2, 2016

Accepted: January 24, 2017

Published: January 24, 2017

to ES cells, iPSCs pose no ethical or immunological hazard.³ Moreover, the patient-specific iPSCs carry the same genetic information on the patients with CVD, which can play an important role in cardiac regeneration and differentiation and therefore can provide a good source for investigation of the effect of different factors on cardiac differentiation in patients.

Our group and others have shown that surface topography and substrate stiffness could considerably affect the cell–matrix interaction, morphology, and therefore cell fate.^{4,5} For instance, aligned fibers and nanofibers enhanced cardiac differentiation of stem cells in comparison to randomly oriented ones.^{6,7} Several studies have shown that 2D electrospun nanofibrous scaffolds can augment cardiac differentiation and proliferation through mimicking the *in vivo* niche of cardiomyocytes.^{8,9} Like an extracellular matrix (ECM), electrospun nanofibrous scaffolds can increase the surface-to-volume ratio resulting in more surface area available for cell culture and differentiation.¹⁰ Moreover, it has been shown that surface modification of scaffolds facilitates cell adhesion, proliferation, and differentiation of stem cells into cardiomyocytes.^{7,11}

An electric field is another important factor that can influence cardiac cell differentiation and behavior.¹² For example, an engineered patch of cardiac tissue will need to be able to electrically integrate into the host myocardium so that it can contract synchronously rather than spontaneously.¹³ In the heart, pacemaker cells, such as the atrioventricular (AV) and sinoatrial (SA) nodes create electrical impulses that are relayed throughout the heart by electrical coupling in a unidirectional manner. Transplantation of an engineered graft with poor electrical conductivity could prevent synergistic integration of the transplanted cells with the host myocardium. Recently, much attention has been directed to polyaniline (PANI) due to its excellent electrical conductivity. PANI can be doped from the nonconductive form of emeraldine base into the conductive form of emeraldine salt by protonic acids like Camphor-10-sulfonic acid (β) (CPSA)¹⁴ and has been used to assist in the delivery of electrical pulses.¹⁵ Moreover, among different doped states of the PANI, PANI-CPSA polymer is significantly aligned in the fiber direction, and due to its proper polymeric chain packaging, better interchain charge transfer occurs in PANI-CPSA.¹⁶ As an added effect, these semiconducting polymers could simultaneously support adhesion and proliferation of cardiomyocytes and induce cardiac differentiation.¹⁷ PANI is a widely used polymer in tissue engineering due to its electroactive properties, high stability, and biocompatibility as well as its simple synthesis and low cost.¹⁸ In addition to these qualities, PANI can act as a scavenger of reactive oxygen species (ROS) and can thus alleviate oxidative stress during myocardial injury.¹⁹ One drawback, however, is the mechanical stability of PANI scaffold, which is low for cardiac differentiation and cannot be fabricated alone. Besides PANI, poly(ether sulfone) (PES) nanofibrous scaffolds are other biocompatible materials that can induce mesodermal differentiation.²⁰ However, although PES has the appropriate mechanical stability for differentiation, its electrical conductivity is low. Therefore, we blended PES with PANI to make a scaffold with more mechanical stability for cardiac differentiation and with high electrical conductivity.

In this study, we aimed to investigate the role of unidirectional electrical stimulation in cardiac differentiation of human CVD-patient-specific iPS (CVD-iPS) cells using aligned electroactive nanofibrous PANI/PES scaffolds in comparison to randomly oriented ones. Moreover, we examined the role of

the aligned versus random nanofibrous scaffolds in cardiac differentiation without applying electrical impulses.

2. MATERIALS AND METHODS

2.1. Production of Lentiviral Particles. Lentiviral particles harboring inducible OSKM (LvOSKM) were produced using calcium–phosphate transfection of HEK 293T cells (4×10^6 cells per 10 cm dish) and a mixture of three plasmids including psPAX2 (21 μ g), pMD2.G (10.5 μ g), and TetO-FUW-OSKM (21 μ g) (Addgene plasmid 20328), a doxycycline-inducible lentiviral vector encoding Oct4-E2A-Sox2-P2A-Klf4-T2A-c-Myc as a polycistronic construct. Reverse tetracycline transactivator-expressing lentiviruses (LvM2rtTA) were also acquired for induction of OSKM expression in cells using the plasmid FUW-M2rtTA (Addgene plasmid 20342). GFP-harboring lentiviruses (LvGFP) were generated using the GFP-carrying pWP1 vector as a control for transfection. For virus titration, HEK 293T cells were transduced with different concentrations of LvGFP and analyzed on the FACScan flow cytometer (Becton Dickinson, San Diego, CA, USA).

2.2. Generation of Human CVD-iPSCs. Adult human dermal fibroblast (HDF) cells from the sternum of four Caucasian females with a diagnosis of CVD disease (48–55 years of age) were isolated and cultured according to a previously published protocol.²¹ The patients had been referred to the “Tehran Heart Center” and underwent cardiac surgery. The study was approved by the Tehran Heart Center Research Ethics Board, and informed consent to participate in this study was obtained from all subjects. The patient’s HDF cells (passage four) were seeded at 10^5 cells per 10 cm dish. Two hours later, the first round of transduction was performed by coinfecting the cells with 3×10^6 particles of both LvOSKM and LvM2rtTA viruses (multiplicity of infection [MOI] = 30), in DMEM/F12 medium supplemented with 8 μ g/mL of polybrene and 10% FBS. Three days after the first transduction, the cells were transferred to a 10 cm dish covered by inactivated mouse embryonic fibroblasts (MEFs) in HUES medium [Knockout DMEM (Invitrogen) containing 20% (v/v) Knockout Serum Replacement (KSR) (Invitrogen), 2 mM GlutaMAX (Invitrogen), 100 μ M nonessential amino acids (Lonza), 100 μ M 2-mercaptoethanol (Invitrogen), 50 U/mL penicillin, 50 mg/mL streptomycin, and 10 ng/mL bFGF] supplemented with doxycycline (DOX) at a final concentration of 1 μ g/mL, and the medium was changed every 2 days. Three weeks after transduction, ES cell-like colonies appeared and were dissociated with collagenase type IV (1 mg/mL). The small clumps were then transferred onto a layer of inactivated MEFs in a 24-well plate and were counted as passage one.

2.3. Characterization of Human CVD-iPSCs. **2.3.1. Alkaline Phosphatase and Immunofluorescence Staining.** Alkaline phosphatase (AP) staining was performed with the Leukocyte Alkaline Phosphatase kit (Sigma-Aldrich) according to the manufacturer’s protocol. For immunofluorescence (IF) staining, CVD-iPSCs were fixed with 4% paraformaldehyde (PFA, Sigma-Aldrich) and permeabilized with 0.1% Triton X-100. Incubation with primary antibodies, including Nanog (Santa Cruz Biotechnology), OCT4 (Santa Cruz Biotechnology), SSEA4 (AbCam), and Tra-1-60 (AbCam), was followed by incubation with secondary antibodies and 4',6-diamidino-2-phenylindole (DAPI) staining. Secondary antibodies used were Alexa Fluor 488 donkey antimouse IgG (Invitrogen), goat antimouse IgM Fab'2 (LifeSpan BioSciences), Alexa Fluor 594 donkey antirabbit (Invitrogen), and FITC goat antirabbit IgG (AbCam).

2.3.2. *In Vitro* Differentiation. For embryoid body (EB) formation, the CVD-iPSCs were harvested by collagenase IV, and the clumps of cells were transferred to nontreated, low adhesion six-well plates (SPL Life Sciences Co) in HUES medium without bFGF. After 5 days, EBs were transferred to gelatin-coated plates and cultured in DMEM/F12 supplemented with 3% KSR for 10 more days to examine spontaneous differentiation into the endodermal lineage. For mesodermal lineage differentiation, one-hundred EBs were cultured for 2 weeks in an osteogenic medium consisting of DMEM/F12 supplemented with 10% FBS, 100 nM dexamethasone (Sigma-Aldrich), 50 μ g/mL ascorbic acid, and 10 mM glycerophosphate. Osteogenesis was confirmed by

detection of calcium depositions using Alizarin Red S staining (Sigma-Aldrich). For adipogenesis, the monolayer of CVD-iPSCs was incubated with adipogenic differentiation medium composed of DMEM supplemented with 50 µg/mL indomethacin (Sigma-Aldrich) and 100 nM dexamethasone. Lipids were detected with Oil Red O (Sigma-Aldrich) staining.

2.3.3. Karyotyping. Genetic stability of the generated ES cell-like colonies was determined by karyotyping and G-banding after cell line establishment and during passages according to a previously published protocol.²²

2.3.4. Teratoma Formation. Teratoma formation was evaluated by subcutaneous transplantation of 10⁷ CVD-iPSCs to the dorsal flank of adult nude mice. After 9 weeks, the explants were dissected, fixed in 4% PFA, and embedded in paraffin. Sections were prepared from paraffin-embedded tissues and stained with hematoxylin and eosin.

2.4. Aligned and Random Nanofiber Scaffold Fabrication and Plasma Treatment. The PANI-containing nanofiber scaffold was fabricated using the electrospinning method.²³ Equivalent amounts of PANI (Sigma-Aldrich) and Camphor-10-sulfonic acid (β) (CPSA) (Sigma-Aldrich) (5 mg/mL) were fully dissolved in DMSO (Merck). PES (Ultrason, Germany) was dissolved at a concentration of 25 w/v% in the solution (PANI/CPSA/DMSO) exactly before electrospinning. Fabrication of PES nanofibrous scaffolds was performed by dissolving PES at a concentration of 33 w/v% in DMSO. To fabricate the aligned and random nanofibrous scaffolds, a rotating collector was used at a speed of 3000 and 1500 rpm, respectively. The distance between the needle and the collector was 150 mm for aligned fibrous scaffolds and 100 mm for random fibers and the voltage was kept at 20 kV.

Hydrophilicity of the scaffold surface was increased by oxygen plasma treatment. Surface plasma treatment was performed by a low-frequency plasma generator (40 kHz, Diener Electronics, Germany) at 30 W for 2.5 min.

2.5. Scaffold Characterization. **2.5.1. Morphology Study.** The surface morphology of the nanofibrous scaffolds and the cells cultured on the scaffold was determined using scanning electron microscopy (SEM). After the cells cultured on the scaffold were washed with 1× PBS, the samples were fixed with 3% glutaraldehyde for 35 min and exposed to consecutive dehydrations in graded ethanol solutions. The samples were left to dry at room temperature (RT) and then mounted on aluminum stubs to spot gold–palladium on them. Images were captured at an accelerating voltage of 15 kV using a scanning electron microscope (VEGAI, TESCAN, Czech Republic). The average diameter of the nanofibers was determined from SEM images from at least 140 randomly selected fibers, and the distribution of angles was chosen in the range of -90° to $+90^\circ$ using image analysis software (ImageJ, NIH, USA). The average values were described with standard deviation ($\theta \pm SD$).

2.5.2. Contact Angle Measurement. The hydrophilicity of the electrospun scaffolds was measured before and after plasma treatment by a contact angle goniometer (Kruss G10, Germany). The average value of the water contact angle of the four droplets was described with standard error ($\theta \pm SE$).

2.5.3. ATR-FTIR Spectroscopy. To analyze the surface chemistry of the scaffolds, attenuated total reflectance-Fourier transform infrared ATR-FTIR spectroscopy was performed using a spectrometer (Bruker Equinox 55) equipped with ATR diamond accessory over a range of 4000–400 cm⁻¹.

2.5.4. Mechanical Properties. The scaffold specimens were prepared with dimensions of 10 × 30 × 0.05 mm³. Tensile properties of the fabricated scaffold were assessed by a universal testing machine (SANTAM) at 10 mm/min traverse speed at RT.

2.5.5. Electrical Properties. The electrical conductivity of dry and hydrated scaffolds was measured using the four-point probe method, elaborated by van der Pau.²⁴ Concisely, after a voltage was applied, the correspondent electrical current was achieved in both directions, parallel and perpendicular to the direction of aligned fibers. Then electrical conductivity was estimated according to the following formula:

$$\sigma \left(\frac{S}{\text{cm}} \right) = \left(2.44 \times \frac{10}{S} \right) \times \left(\frac{I}{E} \right)$$

Where σ is the conductivity, S is the sample side area, I is the current passed through the outer probes, and E is the voltage drop across the inner probe.²⁴ To distinguish any alterations in the electrical conductivity of the scaffold after exposure to cell culture, the fabricated scaffolds were incubated in culture medium at 37 °C and 5% CO₂ for 6 days. After being washed twice with distilled water, the scaffolds were dried at RT before the electrical current was obtained.

2.5.6. 3-(4,5-Dimethylthiazol-2-yl)-2,5-diphenyltetrazolium bromide (MTT) Assay. The viability of the CVD-iPSCs on the fabricated scaffolds was assessed by MTT assay. Briefly, 10³ cells were seeded per well of a 96-well plate with and without the sterilized scaffold. The cell group cultured on the plate was determined as the control group. After a given time, the cell culture medium was discarded and the cells were incubated with 100 µL of 0.5 mg/mL MTT dye solution (Sigma-Aldrich, Cat. R8755). The supernatant was removed, and the formazan crystals that formed in the cells were dissolved in 100 µL of DMSO, and the plates were then analyzed using an ELISA plate reader (BioTek) at 570 nm.

2.6. Bioreactor Design and Manufacturing. An eight-well bioreactor was designed to induce electrical stimulation using 3D CAD design software (SOLIDWORKS, USA) as depicted in Figure 1A. The bioreactor was manufactured from Plexiglas [poly(methyl methacrylate) (PMMA)] by carving out the wells with a CNC router (C.R. Onsrud, Inc., USA). One pair of stainless steel (316) electrodes (diameter, 1.4 mm; length, 25 mm) was inserted on either side of the bottom of the well (Figure 1B, 1). Each electrode in each well was connected to the outside via a pin-shaped interface (Figure 1B, 2). A square-shaped fixative manufactured from Plexiglas was applied to uniformly connect the fabricated scaffolds to the electrodes. To fasten the Plexiglas fixative onto the scaffold, a pair of M4 spacers was inserted at the base of each well (Figure 1C). The bioreactor was sterilized by γ -radiation or by autoclaving before use. After the cells were seeded in the bioreactor, it was put in a CO₂ incubator and connected to a function/arbitrary waveform generator (RIGOL) to generate electrical pulses (Figure 1D).

The electrical behavior of the system in each well of the bioreactor was determined by an electrochemical impedance spectroscopy (EIS) analyzer (FRA/EIS, IviumStat) equipped with IviumSoft software. The EIS spectra were recorded over a frequency range of 10³–10⁶ Hz, with input voltages of 500 and 1000 mV.

2.7. Cardiac Differentiation and Electrical Stimulation. The human CVD-iPSCs were cultured as a monolayer in MEF-conditioned HUES medium in different experimental groups described in Table 1. Four days later, differentiation medium (50 µg/mL Activin A, 10 µg/mL bFGF, and 1% KnockOut Serum Replacement in RPMI/B27-insulin) was added to the cells according to a previously published protocol.²⁵ Additionally, the cells cultured in the bioreactor were exposed to a square-wave field (with the frequency of 1 Hz for 2 ms and 50 mV/cm) that is similar for native myocardium for 1 h/day, over a 15-day time period, which is used in several previous studies.^{26,27} As a control, we used ESC line HS (obtained from the Royan Institute) for culture on the aligned and random nanofibrous scaffolds in the presence of the various differentiation conditions.

2.8. Conventional and Quantitative PCR (qPCR). The cell-seeded nanofibrous scaffolds were subjected to vigorous pipetting in 1 mL of RNX-plus (Cinnagen) and after the scaffolds were dissolved, total RNA was extracted according to the manufacturer's protocol. Total RNA was subjected to reverse transcription using RevertAid First Strand cDNA Synthesis Kit (Thermo Scientific) as described in the kit protocol. Real-time PCR was performed using the SYBR Premix Ex TaqII kit (Takara) on a Thermocycler Rotor-Gene6000 (Corbett Research). Primer sequences are listed in the Supporting Information (Table S1). Generic threshold and PCR efficiencies of each reaction were determined using the LinReg PCR software.²⁸ For measuring relative gene expression, the C_t values of the target genes were normalized to β -actin gene expression and the fold changes of expression were calculated using the following formula:

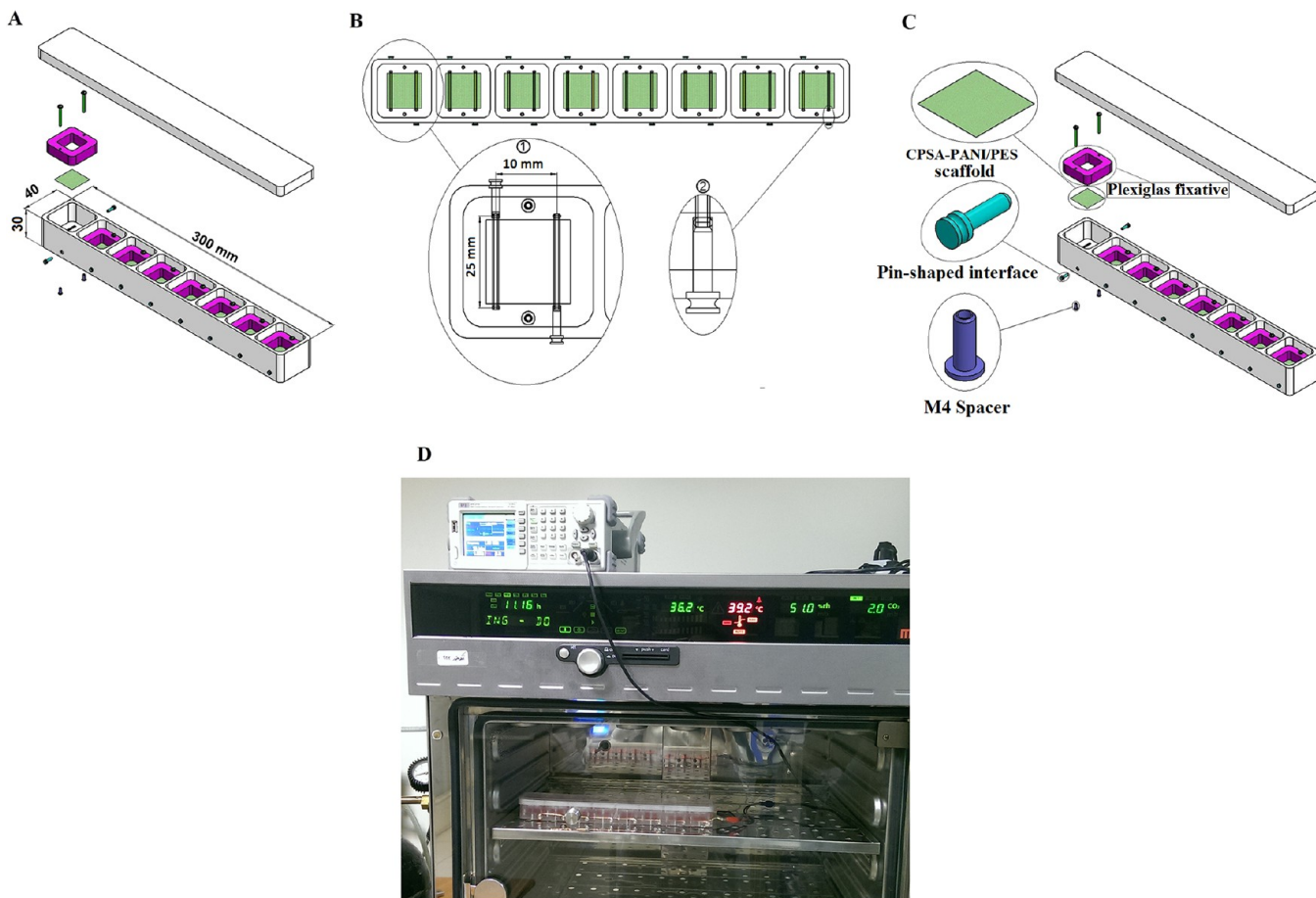


Figure 1. Bioreactor structure. (A) Schematic design of the bioreactor using SOLIDWORKS 3D CAD Software. (B) (1) Structure of a single chamber of the bioreactor and position of electrodes. (2) Pin-shaped interface connecting the electrodes to the electrical pulses. (C) Schematic showing the position of Plexiglas fixative, scaffold, pin-shaped interface, and M4 spacer in each chamber of the bioreactor. (D) Connection of the bioreactor to a function/arbitrary waveform generator in a CO₂ incubator.

$$R = \frac{(E_{\text{target}})^{\Delta Ct_{\text{target}}(\text{Mean normal} - \text{Mean sample})}}{(E_{\text{ref}})^{\Delta Ct_{\text{ref}}(\text{Mean normal} - \text{Mean sample})}}$$

Where R is the relative expression ratio, and E refers to real-time PCR efficiencies for each primer.²⁹

2.9. Flow Cytometry. The CVD-iPS-derived cardiomyocyte-like cells were trypsinized, and the single cells were harvested by centrifugation. The cells were permeabilized with 0.25% Triton X-100 for 10 min and then incubated overnight with anticardiac troponin T antibody (cTnT; AbCam). The cells were washed twice with 1× PBS, incubated with antimouse immunoglobulin/FITC rabbit F (ab') 2 (1:200; Dako) for 30 min, and analyzed using the FACScan flow cytometer (Becton Dickinson, San Diego, CA, USA). The data were analyzed using FlowJo software, and the percentage of cTnT+ cells was calculated.

2.10. Cell Orientation and Immunofluorescence Staining. For IF staining, the cardiomyocyte-like cells derived from CVD-iPS were fixed with 4% paraformaldehyde (PFA, Sigma-Aldrich) and then permeabilized with 0.1% Triton X-100. Incubation with primary antibodies, including α-Actin (Santa Cruz Biotechnology), and cTnT (AbCam) was followed by incubation with secondary antibodies and 4',6-diamidino-2-phenylindole (DAPI) staining. Secondary antibodies used were goat antimouse FITC (AbCam) goat and antimouse IgG (Thermo Fisher Scientific).

Cell orientation analysis was determined using the Fiji directionality plugin. To evaluate the orientation distribution of cytoskeleton fibers, results from four different groups (namely BSD1, SD1, BSD2, and SD2) were analyzed by plotting means. Orientations were quantified by

setting 0° as the cell orientation parallel to the electrical stimulation direction and 90° as that perpendicular to the direction.

2.11. Statistical Analysis. Statistical analysis of real-time PCR was performed using the Relative Expression Software Tool (QIAGEN) with PCR efficiency.²⁹ The statistical significance of expression ratios was analyzed by permutation tests and the standard error calculated using the complex Taylor algorithm.

In the other experiments, one-way ANOVA was carried out to determine the significant variation between treated cell groups in different differentiation conditions. Bonferroni's post hoc test was used to measure statistical significance.

3. RESULTS

3.1. Generation and Characterization of Human CVD-iPSCs. Successful lentiviral production and transduction were confirmed by visualization of GFP expression in the transfected HEK293T and HDF cells, respectively (Figure S1).

To generate human CVD-iPSCs, HDF cells derived from a 50-year-old Caucasian female were simultaneously transfected with DOX-inducible LvOSKM and LvM2rtTA plasmid containing particles (Figure 2A,B). Three weeks after infection, ES cell-like colonies with distinctive borders were detected (Figure 2C). The colonies were picked and expanded on mouse embryonic fibroblast (MEF) feeder cells in HUES medium 30 days post-infection.

The generated CVD-iPSCs showed high alkaline phosphatase activity (Figures 2D and 2E). The expression of endogenous

Table 1. Experimental Groups with Different Culture Conditions^a

group	factor			
	electrical stimulation	aligned nanofibrous scaffolds	random nanofibrous scaffolds	differentiation medium
BSD1	+	+	—	+
BSD2	+	—	+	+
SD1	—	+	—	+
SD2	—	—	+	+
BSH1	+	+	—	—
BSH2	+	—	+	—
SH1	—	+	—	—
SH2	—	—	+	—
GH	—	—	—	—
PBSD1	+	+	—	+
PBSD2	+	—	+	+
ESBSD1	+	+	—	+
ESBSD2	+	—	+	+

^aAbbreviations. BSD1: cells cultured in the bioreactor on the aligned nanofibrous PANI/PES scaffolds using differentiation medium and electric pulses 1 h/day for 15 days. BSD2: cells cultured in the bioreactor on the random nanofibrous PANI/PES scaffolds using differentiation medium and electric pulses 1 h/day for 15 days. SD1: cells cultured on the aligned nanofibrous PANI/PES scaffold with differentiation medium. SD2: cells cultured on the random nanofibrous PANI/PES scaffold with differentiation medium. BSH1: cells cultured in the bioreactor on the aligned nanofibrous PANI/PES scaffold with HUES medium and electrical pulses 1 h/day for 15 days. BSH2: cells cultured in the bioreactor on the random nanofibrous PANI/PES scaffold with HUES medium and electrical pulses 1 h/day for 15 days. SH1: cells cultured on the aligned nanofibrous PANI/PES scaffold with HUES medium. SH2: cells cultured on the random nanofibrous PANI/PES scaffold with HUES medium. GH: cells cultured on gelatin-coated plates with HUES medium. PBSD1: cells cultured in the bioreactor on the aligned nanofibrous PES scaffolds using differentiation medium and electric pulses 1 h/day for 15 days. PBSD2: cells cultured in the bioreactor on the random nanofibrous PES scaffolds using differentiation medium and electric pulses 1 h/day for 15 days. EBSD1: ES cells cultured in the bioreactor on the aligned nanofibrous PANI/PES scaffolds using differentiation medium and electric pulses 1 h/day for 15 days. EBSD2: ES cells cultured in the bioreactor on the random nanofibrous PANI/PES scaffolds using differentiation medium and electric pulses 1 h/day for 15 days.

pluripotent stem cell markers including OCT4, NANOG, SSEA4, and TRA-1–60 was also detected in the reprogrammed cells by IF staining (Figure 2F). In addition, the expression of stem cell markers was confirmed at the transcript levels by RT-PCR (Figure 2G). At the point at which the cells were analyzed, the polycistronic cassette encoding the OSKM transgenes had no longer been expressed as a result of withdrawing DOX (Figure 2H) meaning that the expression of endogenous OSKM genes were switched on and replaced with the expression of exogenous ones. Moreover, G-band karyotyping showed that the generated cells maintained their chromosomal integrity during reprogramming and did not exhibit any chromosomal abnormalities during passages (Figure 2I).

To confirm the pluripotency of the ES cell-like colonies, the iPS cell-derived EBs were directed to form the three-germ layer cell lineages in vitro (Figure 3A). Morphologically, some of the attached EBs assumed neuron-like shapes with obvious projections (Figure 3B,C). Osteogenic differentiation was demonstrated by massive calcium deposits as detected by Alizarin Red

staining (Figure 3D). In the adipogenic medium, adipocyte differentiation was confirmed by Oil Red O staining and visualization of numerous intracellular lipids (Figure 3E). Moreover, RT-PCR of the differentiated EBs confirmed the expression of endodermal genes such as FOXA2 and SOX17; mesodermal gene expression as shown by BRACHYURY; and ectodermal gene expression including MAP2 and PAX6 (Figure 3F). As an additional assay to assess pluripotency, the CVD-iPSCs were injected subcutaneously into the dorsal flanks of adult nude mice, and teratomas were formed within 6–8 weeks after transplantation. Among the 21 ESC-like colonies that formed, histological analysis revealed that two of those lines (hereafter named as CVD-hiPS#9 and CVD-hiPS#12) successfully formed teratomas (Figure 3G).

3.2. Scaffold Characterization. The SEM images of the aligned nanofibrous CPSA-PANI/PES scaffold revealed that the average diameter of the aligned and random nanofibers was 294 ± 66 nm and 267 ± 67 nm, respectively, Figure 4A and B. Alignment of nanofibers was identified using statistical analysis of the angles of the nanofiber in comparison to their major axis. The results showed that the angles of over 82% of the fibers in the aligned fibrous scaffolds were from -30° to 30° compared to their major axis (Figure 4C), while the fibers in random fibrous scaffolds showed an almost equal distribution of different angles (Figure 4F). SEM micrographs of human CVD-iPSCs 5 days and 25 days after seeding on the aligned and random scaffolds are shown in Figure 5. Moreover, the average diameters of the aligned and random PES nanofibers were 275 ± 64 nm and 274 ± 92 nm, respectively (Figure S2).

ATR-FTIR spectra for PES and PANI/PES scaffolds as well as powder material of PANI are shown in Figure 6. The original bands of PES were observed at 1242 cm^{-1} (stretching of aromatic ring), 1489 cm^{-1} (stretching of C–C bands), and 1580 cm^{-1} (stretching of benzene ring) in both PES and PANI/PES scaffolds. Moreover, another characteristic peak of PES was observed with PES and PANI/PES scaffolds as a result of $-\text{SO}_2^-$ groups stretching at 1320 cm^{-1} .³⁰ The peak arising from ether C–O stretching appeared at 1100 cm^{-1} with PES and PANI/PES scaffolds.³¹ The peaks at 1650 and 1655 cm^{-1} , which were reported with PES component,³² represented in PES and PANI/PES scaffolds, respectively. Also, the C–H stretching peak at 3093 cm^{-1} was observed in the PES and PANI/PES scaffolds.³³ The aromatic C=C stretching deformation of the benzenoid and quinoid rings in PANI was observed at 1585 and 1492 cm^{-1} , respectively.³⁴ The typical characteristic band of PANI powder at 1297 cm^{-1} related to the stretching vibration of C–N³⁵ was shifted to 1309 cm^{-1} here. The presence of $-\text{SO}_3^-$ band at 1039 cm^{-1} confirmed the doped type of PANI by CPSA.^{34,36} The peak at 832 cm^{-1} confirmed the out-of-plane hydrogen deformation of aromatic rings in PANI structure,³⁷ and the out-of-plane vibrations of multisubstitution on the benzene groups of PANI were observed at 1007 and 955 cm^{-1} .³⁸ The corresponding peaks at 1007 and 955 cm^{-1} were confirmed with PES and PANI/PES scaffolds as a presence of benzene groups. Moreover, the peak at 1670 cm^{-1} was attributed to the imino group in the PANI and PES/PANI scaffold.³⁹ The other specified peak with PANI powder was reported at 3293 cm^{-1} assigned to N–H stretching⁴⁰ that was shifted to 3255 cm^{-1} with PANI/PES scaffold as a result of interaction between PES and PANI components.

Contact angle measurements showed that the hydrophilicity of both the PANI/PES and PES scaffolds increased greatly after treatment with plasma. The scaffold was much less hydrophilic before plasma treatment (Table S2 and Figure S3).

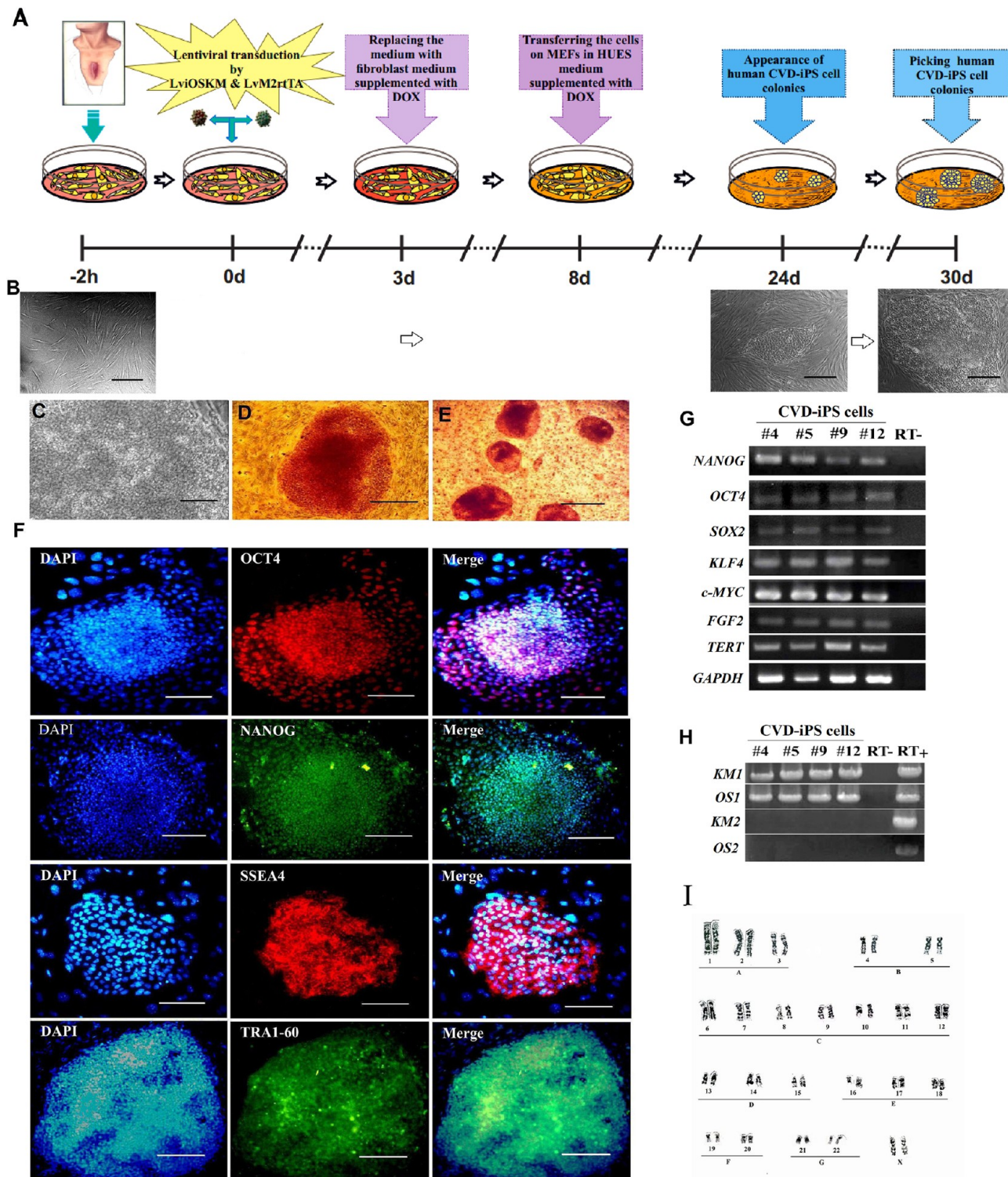


Figure 2. Generation and characterization of human CVD-iPS cell colonies. (A) Time course of human CVD-iPS cell establishment. (B) Morphology of the cells corresponding to the days mentioned in panel A. (C) Magnified view of an undifferentiated CVD-iPS cell colony demonstrating high nucleus-to-cytoplasm ratios and conspicuous nucleoli. (D, E) Alkaline phosphatase staining of the colonies. (F) Immunofluorescence staining of pluripotency markers including OCT4, NANOG, SSEA4, and Tra1–60. (G) Quantitative RT-PCR analysis of pluripotency markers in the generated CVD-iPSCs 30 days after transduction. (H) RT-PCR analysis of endogenous expression of *KLF4* and *c-MYC* (*KM1*), *OCT4*, and *SOX2* (*OS1*) and exogenous expression of *KLF4* and *c-MYC* (*KM2*), *OCT4*, and *SOX2* (*OS2*) in the CVD-iPSCs after elimination of DOX from the HUES medium. (I) G-band karyotyping showing no chromosomal abnormalities in the cells due to reprogramming. Scale bars = 100 μ m (B–D, F) and 200 μ m (E).

The tensile testing of electrospun CPSA-PANI/PES nanofibers showed significant changes in some mechanical properties of the nanofibers due to O₂ plasma treatment.⁴¹ Either way, the mechanical properties of the fabricated scaffold with or without

O₂ plasma treatment were appropriate for cardiac differentiation, but the mechanical properties of random nanofibrous scaffolds were reduced significantly in comparison to aligned nanofibrous scaffolds (Figure S4 and Table S3).

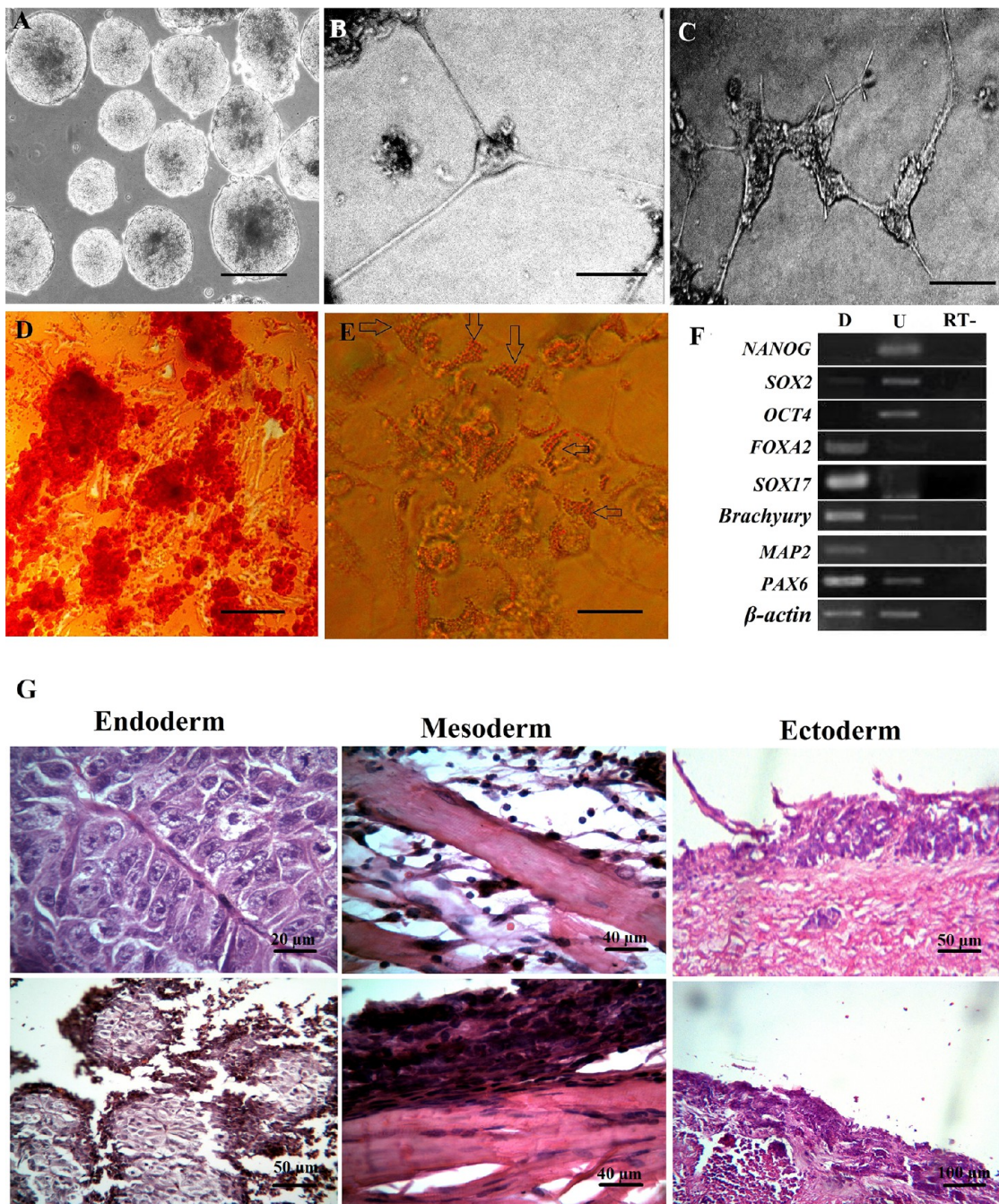


Figure 3. Pluripotency of the human CVD-iPSCs in vitro and in vivo. (A) EB formation in suspension culture. (B, C) Neuron-like morphology of cells after spontaneous differentiation of the EBs. (D, E) Alizarin Red S and Oil Red O stains for osteogenic and adipogenic differentiation, respectively. (F) RT-PCR for detecting the markers of the embryonic-germ layers and pluripotency markers in the differentiated, D, and undifferentiated, U, human CVD-iPSCs. (G) Histological analysis of teratomas derived from the human CVD-iPSCs. Scale bars = 100 μ m (A, C–E) and 50 μ m (B).

The electrical conductivity of the scaffold was measured by utilization of a four-point probe method. The values of electrical conductivity were calculated as $5.7 \times 10^{-4} \pm 0.2$ S/cm, $2.3 \times 10^{-5} \pm 0.08$ S/cm, and 3.8×10^{-5} S/cm by applying the electric current in parallel and perpendicular orientations to the direction of the aligned fibers and to random fibers, respectively. The electrical conductivity of PES scaffolds was calculated as $6.58 \times 10^{-16} \pm 0.06$ S/cm. The scaffolds did not show any change in electrical resistance after 144 h of exposure to the cell culture medium.

Scaffold biocompatibility was tested by MTT assay. The data showed that the viability of human CVD-iPSCs cultured on the

aligned and random nanofibrous scaffolds was approximately equal to the viability of cells cultured on the plates until day 4. The results of MTT on day 5 and 6 showed a significant increase in cell proliferation on the nanofibrous scaffolds in comparison to control group. Moreover, there was no significant difference in cell proliferation between the cells cultured on aligned scaffolds and those on randomly oriented scaffolds (Figure S4).

3.3. Characterization of the Electrical Stimulation System in the Bioreactor. As depicted in Figure S5A, the EIS data were correlated to an equivalent circuit of “Randles cell”, in which the elements of R_s and R_p represent the solution resistance and the polarization resistance (or the electrode’s resistance

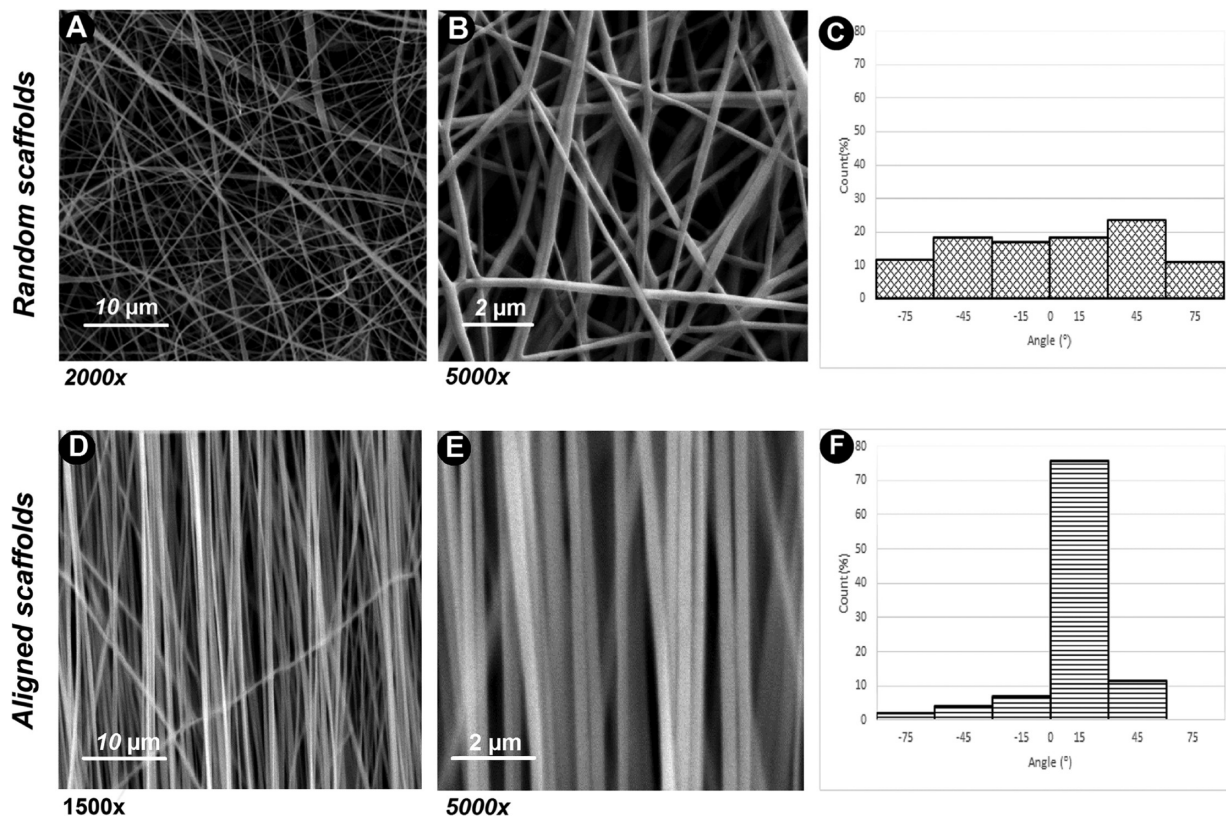


Figure 4. SEM images of (A, B) random and (D, E) aligned CPSA-PANI/PES electrospun nanofibers at different magnifications. Histograms of the fiber angle distributions for (C) random and (F) aligned CPSA-PANI/PES nanofibers.

to corrosion), respectively. The constant-phase element (CPE) is a double layer capacitance related to a nonideal double layer capacitor in the electrode (with ideality η coefficient). The estimated values of the equivalent circuit parameters are listed in Table 2. The Nyquist plots for the electrodes in pulsing buffer and cell culture medium with perturbation voltages ranging from 500–1000 mV are shown in Figure S5B. The results showed that R_p for the electrode in both electrolytes had appropriate resistance to galvanic corrosion.

3.4. Cell Orientation and Immunofluorescence Staining. After 21 days, the cells cultured on the scaffolds were fixed and then stained using α -actin and cTnT antibodies. In the BSD1 group, the highest percentage of cytoskeletal fibers were oriented in the direction of electrical stimulation and fibers, whereas in the SD1 group, the number of cytoskeletal fibers oriented in the direction of aligned fibers reduced in comparison to the BSD1 group. In the BSD2 group, a reduction in the number of cells oriented in direction of electrical stimulation was observed in comparison to BSD1, but this reduction was not significant in comparison to SD1. Lack of external stimuli in the SD2 group led to cell spreading on the surface of the scaffold and therefore a reduction in the number of cells per cm^2 (Figure 7).

3.5. Flow Cytometry Assay. The ability of the human CVD-iPSCs to differentiate into cardiomyocytes was investigated in different conditions. Differentiation efficiencies were quantified by cardiac TnT staining and subsequent flow cytometry (Figure 8).

Flow cytometry demonstrated that the different cell culture conditions effectively influenced the ability of the human CVD-iPSCs to differentiate into cardiomyocyte-like cells. On the basis of the results, the highest number of differentiated cTnT+ cells (~85%) was obtained when the cells were cultured

on the aligned nanofibrous scaffolds and electrically stimulated in the bioreactor (unidirectional electrical stimulation) in the presence of cardiomyocyte-inducing factors (BSD1 group). The cTnT+ cell percentage was reduced significantly to 73.7% when we used random nanofibrous scaffolds (BSD2) (multidirectional electrical stimulation) instead of the aligned-oriented ones. Similar results were found when electrical impulses were applied on aligned (BSH1 = 64.5%) and random (BSH2 = 53.6%) nanofibrous scaffolds and the cardiomyocyte-inducing factors were removed. Interestingly, the cTnT+ cell percentage difference between the groups cultured on aligned (SD1 = 72.3% and SH1 = 50.05%) and random (SD2 = 63.6% and SH2 = 43.9%) nanofibrous scaffolds was not significant in the absence of electrical impulses. These results showed that the aligned nanofibers could enhance cardiac differentiation significantly in the presence of electrical impulses. In other words, an exogenous unidirectional electrical signal using aligned nanofibrous scaffolds could increase cardiac differentiation significantly in comparison to multidirectional stimulation using random nanofibers.

The increase in cTnT+ cell percentages was significant in the BSH1 group in comparison to SH1 and SH2 groups, but it was not significant when the BSH2 group was compared with the SH1 and SH2 groups. These results demonstrated that applying electrical stimulation in the absence of differentiation medium could increase cardiac differentiation only when it was applied in a unidirectional manner.

Comparison of the results of the BSD1 (~85%) and BSH1 (64.5%) groups, as well as SD1 (72.32%) and SH1 (50%) groups, showed the promoting effect of the differentiation medium on driving the cells toward the cardiomyocyte lineage.

Moreover, greater numbers of cTnT+ cells in the BSD1 and BSD2 groups than that of the SD1 and SD2 groups, respectively,

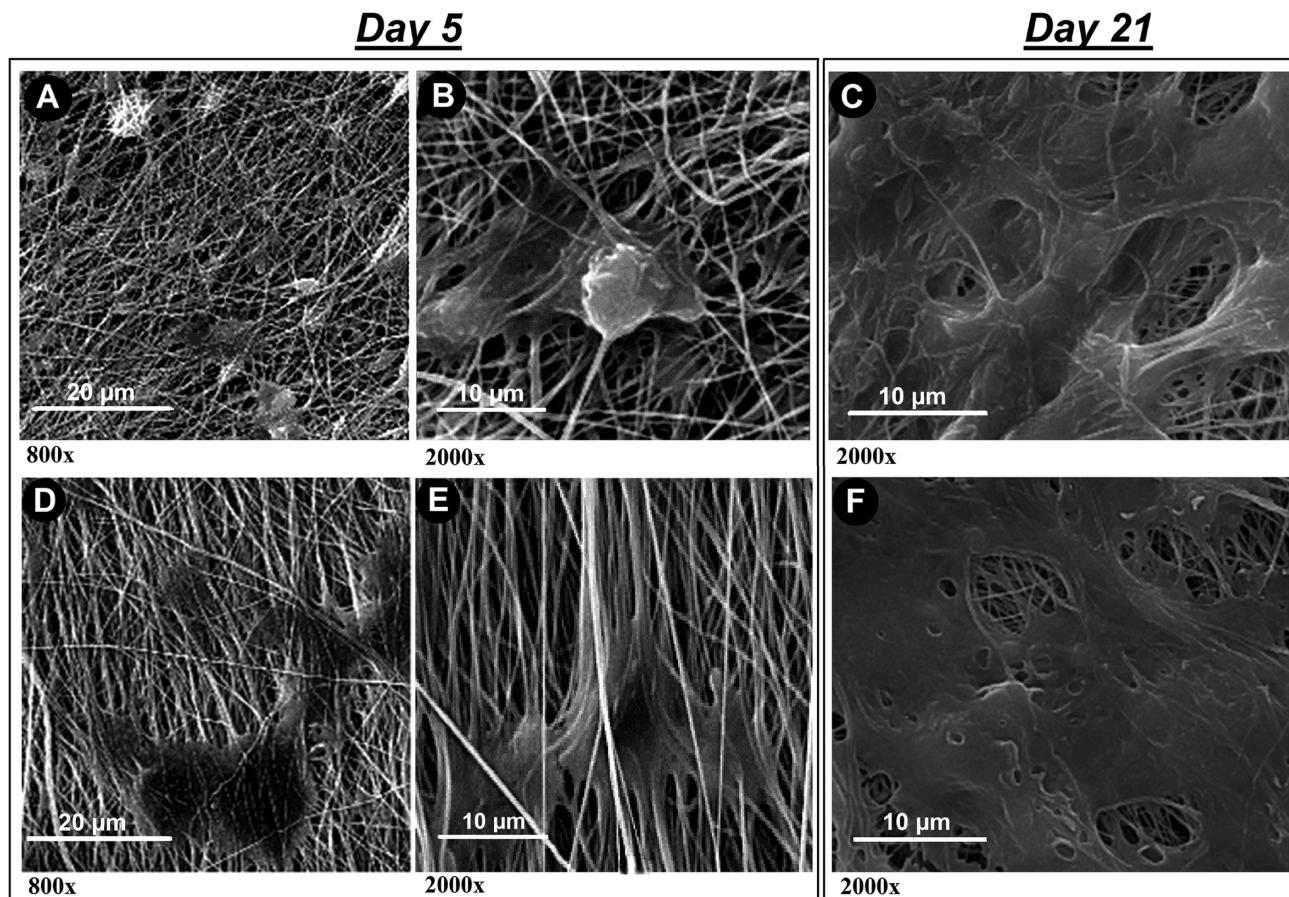


Figure 5. SEM images of human CVD-iPSCs cultured on (A, B) random nanofibrous scaffolds and (D, E) aligned nanofibrous scaffolds 5 days after seeding the cells. The cell morphology on (C) random nanofibrous scaffolds and (F) aligned nanofibrous scaffolds 25 days after seeding the cells.

indicated the augmentative role of electrical impulses on cardiomyocyte differentiation of iPSCs.

These findings demonstrate the inductive role of electrical stimulation, along with conductivity of the scaffolds, in promoting cardiomyocyte differentiation.

3.6. Gene Expression Profiling Assay. Changes in the expression of cardiomyocyte-related genes were evaluated by quantitative RT-PCR to determine the effect of aligned and random nanofibrous scaffolds and electrical impulses at day 21. Here, we used β -actin as an internal control. The cardiac-related transcription factors, including *NKX2.5*, *GATA4*, and *NPPA*, and the cardiac-specific structural gene of *TNNT2* were up-regulated in the various experimental groups (Figure 8). The *p*-values of expression changes in different groups are depicted in Table S4. The most increased ratios of expression of the aforementioned genes were seen in BSD1 group. The *GATA4*, *NPPA*, and *TNNT2* genes showed significant increases in the BSD1 and BSH1 groups compared with the BSD2 and BSH2 groups, respectively. The level of expression of *NKX2.5* increased significantly in the BSD1 group in comparison to the BSD2 group, but it was not significant between the BSH1 and BSH2 groups. On the other hand, the expression ratios of the genes did not significantly change between the SD1 and SH1 groups relative to the SD2 and SH2 groups, respectively. These results were consistent with the flow cytometry results and showed that aligned nanofibers could enhance cardiac differentiation in the presence of electrical stimulation in a unidirectional fashion.

Moreover, the expression of the *TNNT2* and *NPPA* genes increased significantly in the BSH1 group in comparison to SH1

and SH2 groups, but their expression was not increased significantly in the BSH2 group compared with the SH1 and SH2 groups. This demonstrates that electrical stimulation in the absence of differentiation medium can increase cardiac differentiation only when it is applied in a unidirectional manner.

Gene expression of *GATA4* and *NKX2.5* showed that they increased significantly in the BSH1 group in comparison to the SH1 and SH2 groups but did not increase significantly in the BSH2 group compared with the SH1 group. The significantly increased expression of *GATA4* and *NKX2.5* in the BSH2 group relative to the SH2 group may be due to the direct effect of electrical stimulation on expression of these genes.

Thus, these results show that the expression levels of *TNNT2* and *NKX2.5* mRNA in cells cultured on the PES nanofibrous scaffolds were less than the expression levels of the aforementioned genes in the cells cultured on both PANI/PES aligned and randomly oriented nanofibrous scaffolds even in absence of differentiation medium.

To confirm the positive effect of unidirectional electrical pulses on cardiac differentiation, RT-PCR using *TNNT2* and *NKX2.5* primers was performed on the ESC line, Royan HS, cultured on aligned- and random-nanofibrous scaffolds in the presence of differentiation medium and electrical impulses (ESBSD1 and ESBSD2). The data obtained from these experimental groups exhibited similar results as CVD-hiPS (Figure 9).

4. DISCUSSION

In this study, we applied electrical stimulations onto aligned and randomly oriented electroactive scaffolds and investigated their

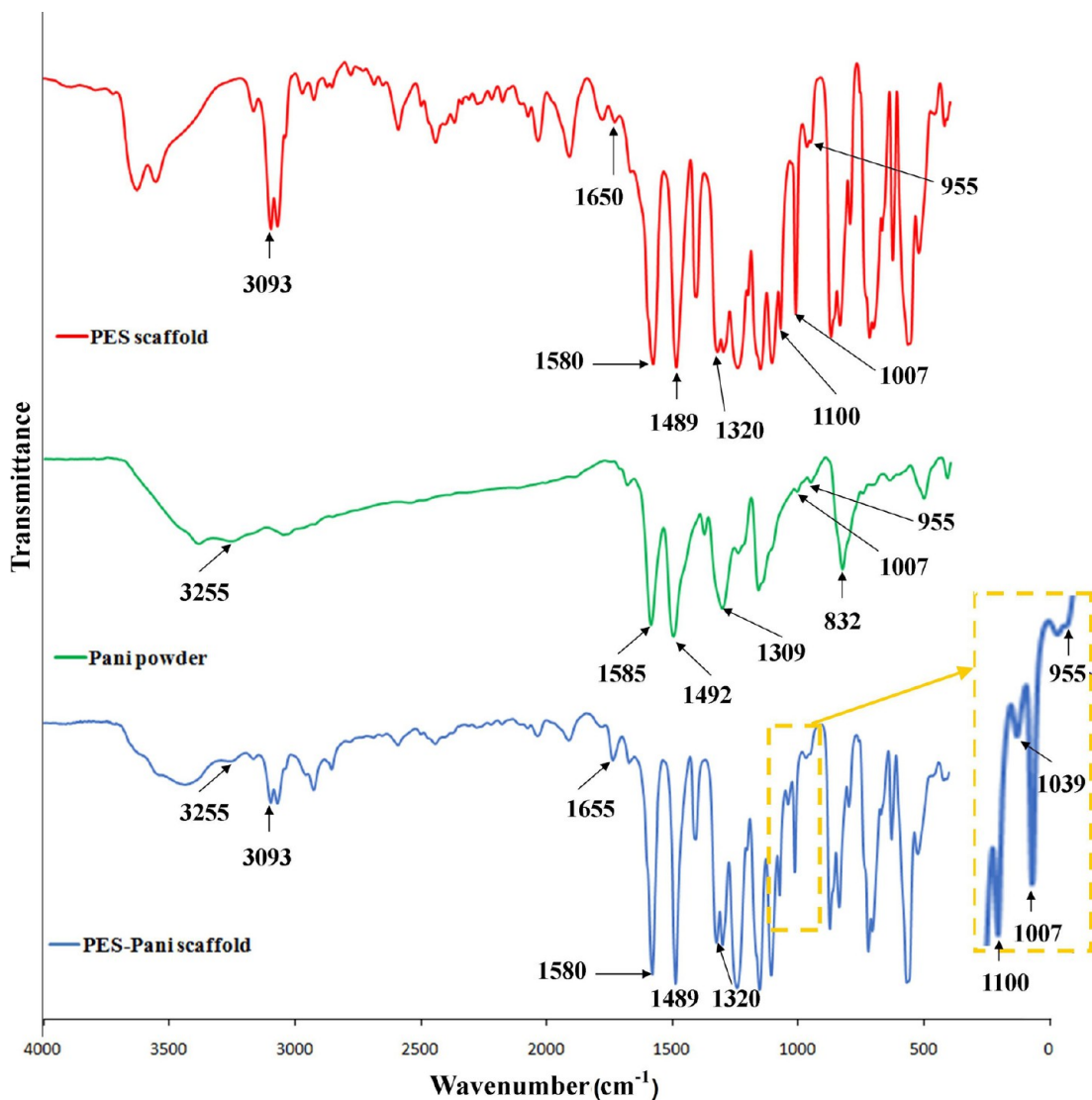


Figure 6. ATR-FTIR spectra of PES nanofibrous scaffold, PANI powders, and CPSA-PANI/PES nanofibrous scaffold.

Table 2. Estimated Values of Equivalent Circuit Parameters^a

electrolytes	input voltage	parameters			
		Rs (Ω) (% error)	CPE (F) (% error)	Rp (Ω) (% error)	η (% error)
HEPES	100 mV	20 \pm 4.95	$1.728 \times 10^{-8} \pm 2.11 \times 10^{-4}$	$4.140 \times 10^{16} \pm 2.56 \times 10^2$	$7.668 \times 10^{-1} \pm 1.01 \times 10^{-4}$
	500 mV	$2.100 \times 10^{11} \pm 2.64$	$4.616 \times 10^{-7} \pm 1.19 \times 10^{-4}$	$1.144 \times 10^{16} \pm 2.86 \times 10^2$	$6.763 \times 10^{-1} \pm 2.39 \times 10^{-4}$
	1000 mV	$1.900 \times 10^{11} \pm 5.59 \times 10^{-1}$	$1.919 \times 10^{-6} \pm 2.49 \times 10^{-4}$	$5.272 \times 10^{14} \pm 1.52 \times 10^1$	$5.558 \times 10^{-1} \pm 3.14 \times 10^{-4}$
cell culture	100 mV	$2.100 \times 10^{11} \pm 4.99$	$1.841 \times 10^{-6} \pm 1.92 \times 10^{-4}$	$3.609 \times 10^{18} \pm 3.91 \times 10^2$	$7.717 \times 10^{-1} \pm 8.82 \times 10^{-5}$
	500 mV	$2.201 \times 10^{11} \pm 3.45 \times 10^{-1}$	$4.631 \times 10^{-6} \pm 4.72 \times 10^{-3}$	$8.536 \times 10^{15} \pm 4.65 \times 10^2$	$6.528 \times 10^{-1} \pm 1.43 \times 10^{-4}$
	1000 mV	$2.220 \times 10^{11} \pm 5.89 \times 10^{-2}$	$6.772 \times 10^{-6} \pm 1.57 \times 10^{-5}$	$1.513 \times 10^{13} \pm 1.18 \times 10^{-1}$	$5.292 \times 10^{-1} \pm 3.49 \times 10^{-4}$

^aAbbreviations. Rs: bulk solution resistance. CPE: constant phase element. Rp: polarization resistance. η : capacitance dispersion.

effects on the differentiation of pluripotent stem cells to cardiomyocytes. The data showed that unidirectional electrical stimulation obtained with the aligned scaffolds drove the cells more efficiently to cardiomyocytes than that of multidirectional electrical stimulation produced by randomly oriented scaffolds.

Recapitulation of the conditions and events leading to cardiac differentiation and maturation is one of the major challenges in cardiac tissue engineering.⁴² It has been previously observed that the more we mimic heart tissue *in vitro*, the higher efficiency of differentiation into cardiomyocytes one achieves. Additionally,

the source of stem/progenitor cells is a critical issue in cardiac regeneration and tissue engineering and it has been shown that genetic factors play important roles in the pathogenesis of CVD. As for patient-specific iPSCs, in addition to solving ethical and immune rejection problems, they also contain the same genetic factors and information as the patients with CVD in which they come from which may play an important role in cardiac regeneration and differentiation. In this study, human iPSCs were generated from patients with CVD (referred here as CVD-iPSCs). Among 21 ESC-like colonies, two lines were characterized as

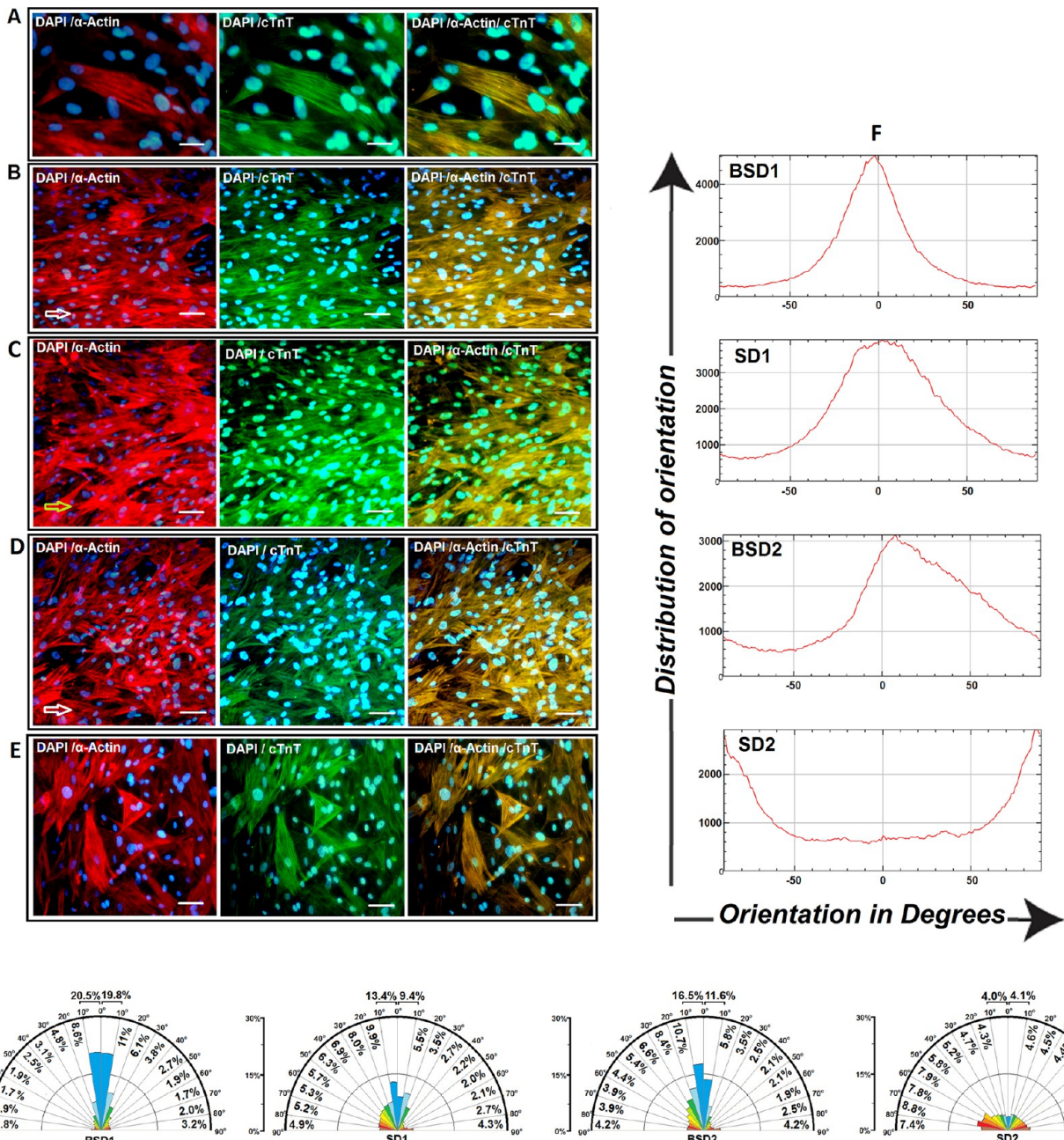


Figure 7. Immunofluorescence staining of cardiac-specific structural including α -actin and cTnT in (A) cardiomyocyte-like cell (zoom in view). The cells cultured on aligned and PANI/PES nanofibrous scaffolds (B) with and (C) without electrical stimulation. The cells cultured on random PANI/PES nanofibrous scaffolds (D) with and (E) without electrical stimulation. (F) Distribution of orientations against orientation of cells in the experimental groups. (G) Quantitative analysis of cellular alignment in the angle of 0–90° in both directions. The white arrows showed the electrical pulse orientation and cyan arrow showed the orientation of fibers in the scaffold. Scale bars = 20 μ m (A) and 100 μ m (B–E).

iPSCs using alkaline phosphatase, immunofluorescence staining, *in vitro* differentiation, karyotyping, and teratoma formation.

In this study, our research group attempted to mimic the native niche of cardiac tissues *in vitro*, which we hypothesized could lead to the generation of a higher number of cardiomyocyte-like cells. To test this hypothesis, electrical impulses, similar to those *in vivo*, were applied to the CVD-iPSCs cultured on aligned nanofibrous PANI/PES scaffolds. This acted as an electrically active cell culture system similar to the *in vivo* conditions in the human heart, which has been shown to promote cardiogenesis.^{12,43}

The primary pacemaker cells, which generate the first electrical impulses during embryogenesis, originate from fetal

cardiomyocytes located in the center of sinoatrial node.⁴⁴ It is thought that these electrical impulses are involved in changing cell morphology and therefore involved in cardiogenesis.⁴⁵ Several studies showed that exogenous electrical stimulation promoted the cardiac differentiation of various types of stem cells^{12,43} through changing intracellular ion concentrations,⁴⁶ producing ROS,⁴³ or colocalizing growth factor receptors and lipids in the plasma membrane.⁴⁷ In this work, we applied exogenous electrical impulses using a bioreactor designed to apply electrical stimulation to cells via stainless steel electrodes. A study by Elena Serena et al. on titanium nitride, titanium, and stainless steel as electrodes showed that stainless steel had the

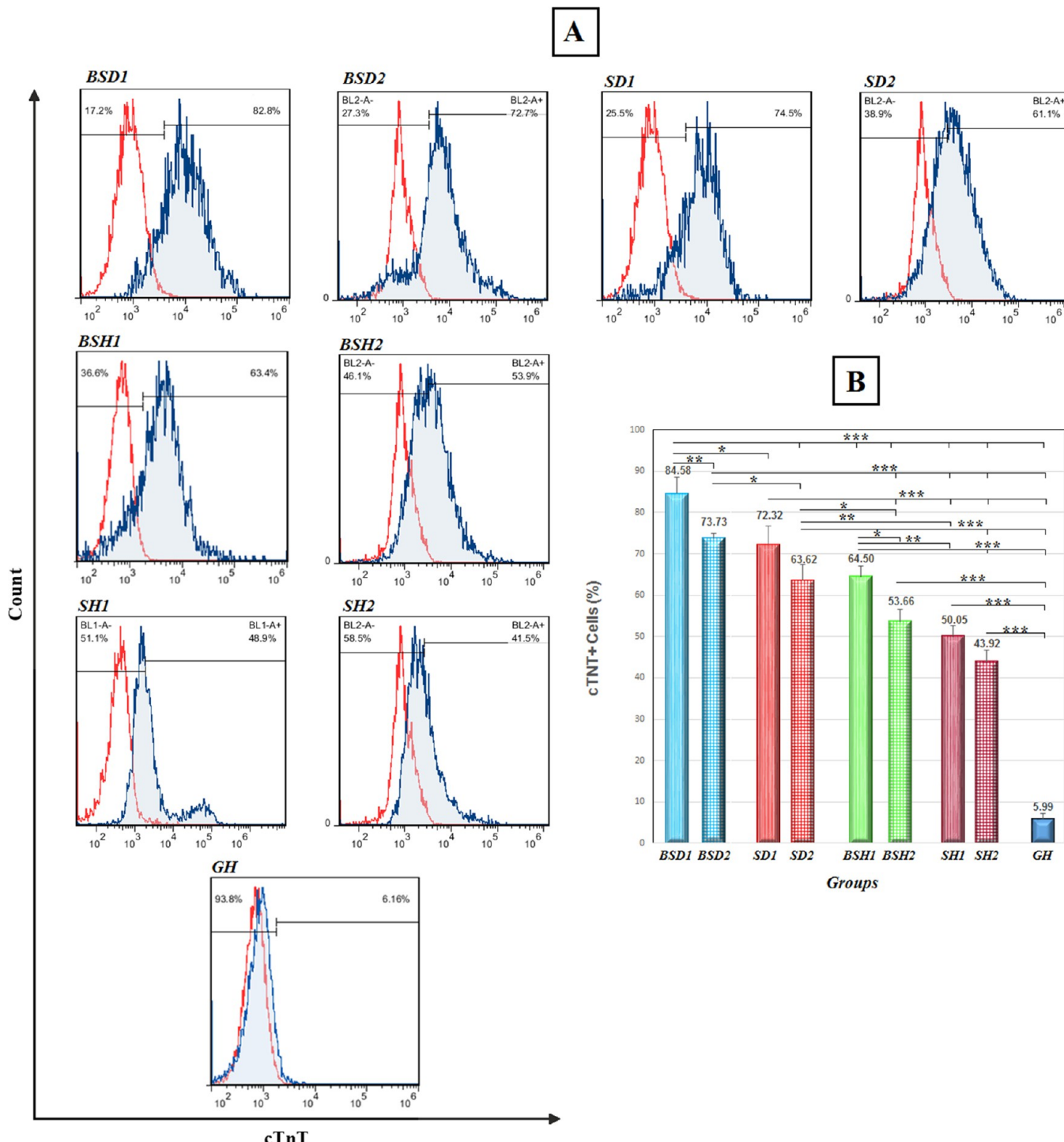


Figure 8. Flow cytometry of cardiomyocytes derived from CVD-iPSCs. (A) Histogram represents one experiment. (B) Statistical analysis of $n = 3$ for each of the different groups showed that different conditions produced varying efficiencies of differentiation of human CVD-iPSCs. (*, $p < 0.05$; **, $p < 0.01$; ***, $p < 0.001$).

lowest polarization resistance with a steady-state current and was suitable for cardiac regeneration.⁴³ Likewise, analysis of the electrical properties of our bioreactor system using EIS showed that it is suitable for cardiac differentiation (Table 2 and Figure S5).

There are some bundles of pacemaker cells in the heart that originate from SAN and pass electrical stimulation through the insulating fibers and cell layers.⁴⁴ During cardiomyogenesis, myocardium needs fast conducting properties to establish adequate heart function in the developing organism. Several

studies showed that conducting polymers can support adhesion and proliferation of cardiomyocytes and can induce cardiac differentiation.^{17,18} Moreover, a previous study showed that the electrical conductivity of the scaffold could synchronize cell contractions of individual cardiomyocyte clusters.¹³ Here, biocompatible PANI/PES scaffolds doped by CPSA were used, which had proper electrical conductivity, and could assist in the delivery of electrical pulses to the cells similar to bundles of pacemaker cells. Our results showed that the electrical

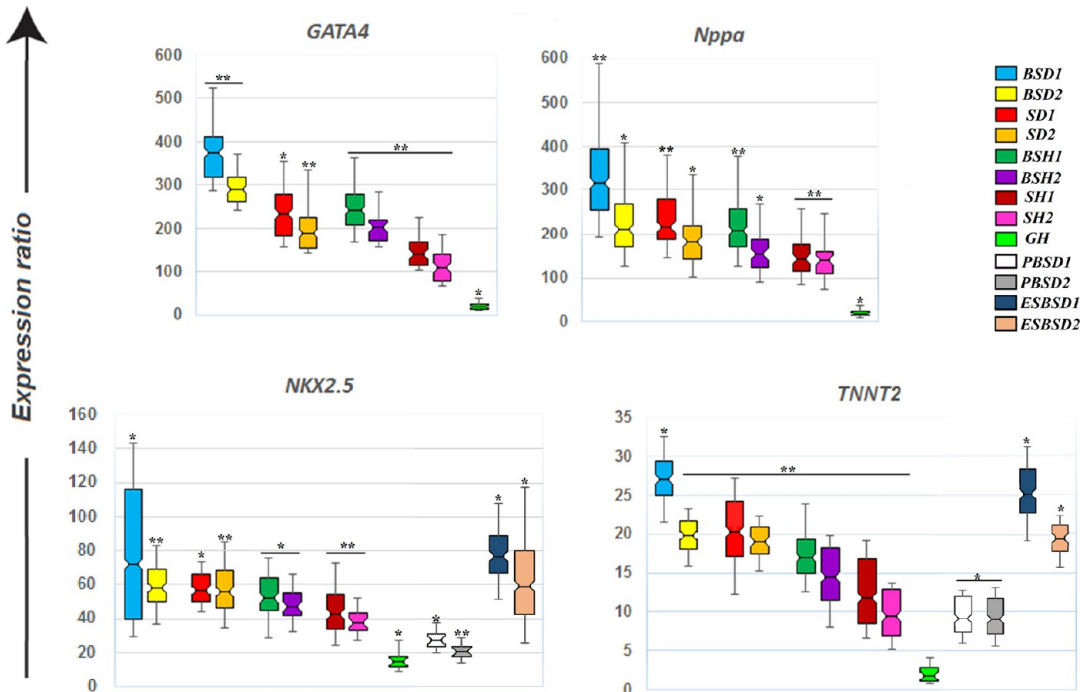


Figure 9. Gene expression levels of cardiac-related transcription factors (*NKX2.5*, *GATA4*, and *NPPA*) and a cardiac-specific structural gene (*TNNT2*) in differentiated groups compared with human CVD-iPS and ES cells (control group for ESBSD1 and ESBSD2 groups). The data are represented with box-and-whisker plots where boxes represent the interquartile range, or the middle 50% of observations and the middle line represents the median gene expression; *, $p < 0.05$; **, $p < 0.01$.

conductivity of PES scaffolds was in the range of electrical insulating materials, whereas the conductivity aligned nanofibrous scaffolds were 15-times greater than random ones, but the conductivity of both of them was in the range of semiconductor materials (10^2 – 10^{-6} S/cm), which is appropriate for tissue engineering purposes.^{15,18} Because of the hydrophobic properties of the surface of these electrospun scaffolds, their surfaces were treated with O₂ plasma. The results of the contact angle assay and ATR-FTIR demonstrated that hydrophilicity of the scaffold surfaces was increased significantly after plasma treatment. It is thought that the conferred hydrophilicity of the O₂ plasma-treated scaffold could facilitate cell adhesion, proliferation, and differentiation.⁴⁸

Scaffold biocompatibility was tested by MTT assay on the cells cultured on aligned and random PANI/PES nanofibrous scaffolds and the cells cultured on the 96-well plates as a control group. MTT assay showed that there was no significant difference in cell proliferation in the groups until day 4. The MTT assay on day 5 and 6 indicated that the cell proliferation rate increased significantly on both aligned and random nanofibrous scaffolds compared to the control group. This increase may be due to the 2D structures of the nanofibrous scaffolds, which recapitulate the ECM of the cells more effectively in comparison to the culture system in the control group.^{9,49}

Here, using electrospinning, the fabricated scaffolds had appropriate chemical (Figure 6) and physical features (Table S3 and Figure S4) for cardiac regeneration.⁴¹

A study showed that aligned electroactive nanofibrous scaffolds synchronized the beating of electrically coupled isolated cardiomyocyte clusters.¹³ In another study, aligned fibers and nanofibers enhanced cardiac differentiation in comparison to randomly oriented ones.⁷ An additional study showed that longitudinally aligned collagen fibers could increase left ventricular function after myocardial infarction.¹¹ Nevertheless, there

are no studies investigating the effect of aligned electrically active nanofibrous scaffolds on cardiac differentiation compared with random electrically active nanofibrous scaffolds. Herein, we compared the effect of these two types of scaffolds on cardiac differentiation in the presence and absence of exogenous electrical impulses. The results showed that the BSD1 group had the highest percentage of the cells with the same orientation. However, the cells with the same direction reduced in the SD2 and BSD2 groups. These results verified the cooperative roles of aligned-oriented nanofibers and electrical stimulation in cell orientation and ultimately in myocardial contractility. Interestingly, the results of flow cytometry for cTnT and RT-PCR for cardiac-related genes showed that using aligned electroactive nanofibrous scaffolds without electrical stimulation could increase cardiac differentiation in comparison to random-ones, but the increase was not significant. However, by applying electrical stimulation a large increase in differentiation was observed with the aligned scaffold, and the expression of *NKX2.5*, *GATA4*, *NPPA*, and *TNNT2* genes increased sharply in comparison with random scaffolds. These findings suggested that unidirectional electrical stimulation is more effective for cardiac differentiation compared with multidirectional electrical stimulation. Moreover, the results of flow cytometry and qPCR for *cTnT* and *NPPA* showed that in the absence of differentiation medium, electrical impulses could increase the expression of the aforementioned genes significantly. However, this was only when applied in a unidirectional manner using aligned electrically active scaffolds. Moreover, further analysis indicated that gene expression for *GATA4* and *NKX2.5* increased during both unidirectional and multidirectional stimulation of the cells. This phenomenon may be due to the regulation of *GATA4* and *NKX2.5* genes directly by electrical stimulation. Electrical pulses promote intracellular ROS production, which in turn induces intracellular Ca²⁺ release.⁴³ Several studies have shown that

signaling by intracellular Ca^{2+} plays a crucial role in cardiac gene expression and differentiation.^{43,50} Intracellular Ca^{2+} can increase cardiac differentiation by increasing *GATA4*.⁵¹ A previous study showed that the *GATA4* and Calcineurin/NFAT pathways could link electrical stimulation to cardiac gene expression.⁵² Therefore, the elevated expression of *GATA4* in the BSH2 group in comparison to the SH2 group might be due to the direct effect of electrical stimulation on *GATA4* up-regulation. As discussed previously, NFAT is another transcription factor whose transcription is directly regulated by electrical stimulation,⁵² which can also directly induce *NKX2.5* expression.

Because the PES scaffolds are electrical insulators, the fibers could not conduct electrical signal to the cells cultured on them. Hence, applying electrical stimulation to the cells cultured on aligned-oriented nanofibrous PES scaffolds could not affect the *TNNT2* and *NKX2.5* expression significantly in comparison to random-oriented ones. Furthermore, the expression levels of aforementioned genes in the cells cultured on random- and aligned-nanofibrous PES scaffolds were less than the cells cultured on the PANI/PES scaffold even in absence of differentiation medium and electrical stimulation. The findings confirm the critical role of electrical conductivity of the cell culture systems on cardiac differentiation. Here, we report for the first time that unidirectional electrical stimulation of cells grown on aligned nanofibrous electrically active scaffolds enhances the cardiogenesis of CVD-iPSCs. This finding is very important for cardiac tissue engineering to be used in regenerative applications.

5. CONCLUSION

The iPSCs used in this study were generated from the fibroblasts of patients with CVD and used as a source of cardiomyocytes for regenerative medicine. Semiconducting aligned and random oriented nanofibrous scaffolds of PANI/PES doped by CPSA were fabricated by electrospinning and then treated with O_2 plasma to increase its surface hydrophilicity. A bioreactor was then designed and manufactured to uniformly transmit electrical impulses to the cells cultured on the O_2 plasma treated PANI/PES scaffold. Application of electrical signals to the aligned electroactive nanofibrous scaffold produced the highest differentiation into cTnT⁺ cells and induced the expression of cardiac-related transcription factors. We believe that these culture conditions nearly mimic the *in vivo* niche of cardiomyocytes in the heart. We have shown that to successfully obtain high levels of cardiomyocytes from iPSCs, providing a semiconductive culture system with electrical stimulation is required. Moreover, the unidirectional electrical stimulation using aligned nanofibrous electrically active PANI/PES scaffolds enhances the cardiomyocyte differentiation of CVD-iPSCs in comparison to multidirectional stimulation using electrically active random oriented scaffolds. The results of this study are important for defining the factors affecting the generation of cardiomyocytes *in vitro* for cell replacement therapies to treat CVD and can help to understand the mechanisms of heart development under the stimulation of cardiac electrical impulses.

■ ASSOCIATED CONTENT

Supporting Information

The Supporting Information is available free of charge on the ACS Publications website at DOI: [10.1021/acsami.6b15271](https://doi.org/10.1021/acsami.6b15271).

GFP expression in transfected HEK293T and HDF cells; SEM images of random and aligned PES nanofibrous scaffolds; images of water droplets in contact with

scaffolds; stress-strain curve of nanofibrous scaffolds; cell viability assessment on PES/PANI scaffolds; electrochemical impedance spectroscopy results of bioreactor electrodes; list of used primers in PCR; contact angle measurement results for PES and PES/PANI nanofibrous scaffolds; tensile test results for PES and PES/PANI nanofibrous scaffolds ([PDF](#))

■ AUTHOR INFORMATION

Corresponding Authors

*E-mail: mohammad.massumi@utoronto.ca. Phone: 416-586-4800 ext. 5361. Fax: 416-586-5130.

*E-mail: shamsa@nigeb.ac.ir. Phone: +982144787414. Fax: +982144787399.

ORCID

Leila Mohammadi Amirabad: [0000-0003-1835-4563](#)

Jalal Barzin: [0000-0002-4860-5805](#)

Notes

The authors declare no competing financial interest.

■ ACKNOWLEDGMENTS

This work was supported by grants from Tehran University of Medical Sciences (Grant No. 91-01-159-17135), Iranian Council of Stem Cell Research and Technology (Project code: 1132), National Institute of Genetic Engineering and Biotechnology (Grant No. M-421), and Stem Cell Technology Research Center.

■ ABBREVIATIONS

PANI, polyaniline

PES, polyethersulfone

CPSA, Camphor-10-sulfonic acid (β)

BSD1, cells cultured in the bioreactor on the aligned nanofibrous scaffolds using differentiation medium and electric pulses 1 h/day for 15 days

BSD2, cells cultured in the bioreactor on the random nanofibrous scaffolds using differentiation medium and electric pulses 1 h/day for 15 days

SD1, cells cultured on the aligned nanofibrous scaffold with differentiation medium

SD2, cells cultured on the random nanofibrous scaffold with differentiation medium

BSH1, cells cultured in the bioreactor on the aligned nanofibrous scaffold with HUES medium and electrical pulses 1 h/day for 15 days

BSH2, cells cultured in the bioreactor on the random nanofibrous scaffold with HUES medium and electrical pulses 1 h/day for 15 days

SH1, cells cultured on the aligned nanofibrous scaffold with HUES medium

SH2, cells cultured on the random nanofibrous scaffold with HUES medium

GH, cells cultured on gelatin-coated plates with HUES medium

PBSD1, cells cultured in the bioreactor on the aligned nanofibrous PES scaffolds using differentiation medium and electric pulses 1 h/day for 15 days

PBSD2, cells cultured in the bioreactor on the random nanofibrous PES scaffolds using differentiation medium and electric pulses 1 h/day for 15 days

ESBSD1, ES cells cultured in the bioreactor on the aligned nanofibrous PANI/PES scaffolds using differentiation medium and electric pulses 1 h/day for 15 days
ESBSD2, ES cells cultured in the bioreactor on the random nanofibrous PANI/PES scaffolds using differentiation medium and electric pulses 1 h/day for 15 days

■ REFERENCES

- (1) *Cardiovascular Diseases (CVDs) Fact Sheet*; WHO: Geneva, 2015.
- (2) Tallawi, M.; Rosellini, E.; Barbani, N.; Cascone, M. G.; Rai, R.; Saint-Pierre, G.; Boccaccini, A. R. Strategies for the Chemical and Biological Functionalization of Scaffolds for Cardiac Tissue Engineering: A Review. *J. R. Soc., Interface* **2015**, *12*, 20150254.
- (3) Tsumaki, N.; Okada, M.; Yamashita, A. iPS Cell Technologies and Cartilage Regeneration. *Bone* **2015**, *70*, 48–54.
- (4) Massumi, M.; Abasi, M.; Babaloo, H.; Terraf, P.; Safi, M.; Saeed, M.; Barzin, J.; Zandi, M.; Soleimani, M. The Effect of Topography on Differentiation Fates of Matrigel-coated Mouse Embryonic Stem Cells Cultured on PLGA Nanofibrous Scaffolds. *Tissue Eng., Part A* **2012**, *18*, 609–620.
- (5) Murphy, W. L.; McDevitt, T. C.; Engler, A. J. Materials as Stem Cell Regulators. *Nat. Mater.* **2014**, *13*, 547–557.
- (6) Khan, M.; Xu, Y.; Hua, S.; Johnson, J.; Belevych, A.; Janssen, P. M.; Gyorke, S.; Guan, J.; Angelos, M. G. Evaluation of Changes in Morphology and Function of Human Induced Pluripotent Stem Cell Derived Cardiomyocytes (HiPSC-CMs) Cultured on an Aligned-nanofiber Cardiac Patch. *PLoS One* **2015**, *10*, e0126338.
- (7) Safaeijavan, R.; Soleimani, M.; Divsalar, A.; Eidi, A.; Ardeshirylajimi, A. Comparison of Random and Aligned PCL Nanofibrous Electrospun Scaffolds on Cardiomyocyte Differentiation of Human Adipose-derived Stem Cells. *Iran J. Basic Med. Sci.* **2014**, *17*, 903–911.
- (8) Zhao, G.; Zhang, X.; Lu, T. J.; Xu, F. Recent Advances in Electrospun Nanofibrous Scaffolds for Cardiac Tissue Engineering. *Adv. Funct. Mater.* **2015**, *25*, 5726–5738.
- (9) Guo, B.; Lei, B.; Li, P.; Ma, P. X. Functionalized Scaffolds to Enhance Tissue Regeneration. *Regener. Biomater.* **2015**, *2*, 47–57.
- (10) Cui, W.; Zhou, Y.; Chang, J. Electrospun Nanofibrous Materials for Tissue Engineering and Drug Delivery. *Sci. Technol. Adv. Mater.* **2010**, *11*, 014108.
- (11) Voorhees, A. P.; Han, H.-C. A Model to Determine the Effect of Collagen Fiber Alignment on Heart Function Post Myocardial Infarction. *Theor. Biol. Med. Model.* **2014**, *11*, 6.
- (12) Hernández, D.; Millard, R.; Sivakumaran, P.; Wong, R. C.; Crombie, D. E.; Hewitt, A. W.; Liang, H.; Hung, S. S.; Pébay, A.; Shepherd, R. K. Electrical Stimulation Promotes Cardiac Differentiation of Human Induced Pluripotent Stem Cells. *Stem Cells Int.* **2016**, *2016*, 1.
- (13) Hsiao, C.-W.; Bai, M.-Y.; Chang, Y.; Chung, M.-F.; Lee, T.-Y.; Wu, C.-T.; Maiti, B.; Liao, Z.-X.; Li, R.-K.; Sung, H.-W. Electrical Coupling of Isolated Cardiomyocyte Clusters Grown on Aligned Conductive Nanofibrous Meshes for Their Synchronized beating. *Biomaterials* **2013**, *34*, 1063–1072.
- (14) Khuspe, G.; Chougule, M.; Navale, S.; Pawar, S.; Patil, V. Camphor Sulfonic Acid Doped Polyaniline-tin Oxide Hybrid Nanocomposites: Synthesis, Structural, Morphological, Optical and Electrical Transport Properties. *Ceram. Int.* **2014**, *40*, 4267–4276.
- (15) Balint, R.; Cassidy, N. J.; Cartmell, S. H. Conductive Polymers: Towards a Smart Biomaterial for Tissue Engineering. *Acta Biomater.* **2014**, *10*, 2341–2353.
- (16) Pouget, J.; Hsu, C.-H.; Mac Diarmid, A.; Epstein, A. Structural Investigation of Metallic PAN-CSA and Some of Its Derivatives. *Synth. Met.* **1995**, *69*, 119–120.
- (17) Bidez, P. R.; Li, S.; MacDiarmid, A. G.; Venancio, E. C.; Wei, Y.; Lelkes, P. I. Polyaniline, an Electroactive Polymer, Pupports Adhesion and Proliferation of Cardiac Myoblasts. *J. Biomater. Sci., Polym. Ed.* **2006**, *17*, 199–212.
- (18) Qazi, T. H.; Rai, R.; Boccaccini, A. R. Tissue Engineering of Electrically Responsive Tissues Using Polyaniline Based Polymers: A Review. *Biomaterials* **2014**, *35*, 9068–9086.
- (19) Gizdavic-Nikolaidis, M.; Travas-Sejdic, J.; Bowmaker, G. A.; Cooney, R. P.; Kilmartin, P. A. Conducting Polymers as Free Radical Scavengers. *Synth. Met.* **2004**, *140*, 225–232.
- (20) Ardeshirylajimi, A.; Hosseinkhani, S.; Parivar, K.; Yaghmaie, P.; Soleimani, M. Nanofiber-based Polyethersulfone Scaffold and Efficient Differentiation of Human Induced Pluripotent Stem Cells into Osteoblastic Lineage. *Mol. Biol. Rep.* **2013**, *40*, 4287–4294.
- (21) Raya, Á.; Rodríguez-Pizà, I.; Navarro, S.; Richaud-Patin, Y.; Guenecéa, G.; Sánchez-Danés, A.; Consiglio, A.; Bueren, J.; Belmonte, J. C. I. A Protocol Describing the Genetic Correction of Somatic Human Cells and Subsequent Generation of iPS Cells. *Nat. Protoc.* **2010**, *5*, 647–660.
- (22) Bayani, J.; Squire, J. A. Traditional Banding of Chromosomes for Cytogenetic Analysis. *Curr. Protoc. Cell Biol.* **2004**, *22*, 22.3.
- (23) Teo, W.-E.; Inai, R.; Ramakrishna, S. Technological Advances in Electrospinning of Nanofibers. *Sci. Technol. Adv. Mater.* **2011**, *12*, 013002.
- (24) Tokarska, M. Evaluation of Measurement Uncertainty of Fabric Surface Resistance Implied by the Van der Pauw Equation. *IEEE Trans. Instrum. Meas.* **2014**, *63*, 1593–1599.
- (25) Lian, X.; Zhang, J.; Azarin, S. M.; Zhu, K.; Hazeltine, L. B.; Bao, X.; Hsiao, C.; Kamp, T. J.; Palecek, S. P. Directed Cardiomyocyte Differentiation from Human Pluripotent Stem Cells by Modulating Wnt/β-Catenin Signaling under Fully Defined Conditions. *Nat. Protoc.* **2012**, *8*, 162–175.
- (26) Llucià-Valdeperas, A.; Sanchez, B.; Soler-Botija, C.; Gálvez-Montón, C.; Prat-Vidal, C.; Roura, S.; Rosell-Ferrer, J.; Bragos, R.; Bayes-Genís, A. Electrical Stimulation of Cardiac Adipose Tissue-Derived Progenitor Cells Modulates Cell Phenotype and Genetic Machinery. *J. Tissue Eng. Regener. Med.* **2015**, *9*, E76–E83.
- (27) Massai, D.; Cerino, G.; Gallo, D.; Pennella, F.; Deriu, M.; Rodriguez, A.; Monteverchi, F.; Bignardi, C.; Audenino, A.; Morbiducci, U. Bioreactors as Engineering Support to Treat Cardiac Muscle and Vascular Disease. *J. Healthcare Eng.* **2013**, *4*, 329–370.
- (28) Ruijter, J.; Ramakers, C.; Hoogaars, W.; Karlen, Y.; Bakker, O.; Van den Hoff, M.; Moorman, A. Amplification Efficiency: Linking Baseline and Bias in the Analysis of Quantitative PCR Data. *Nucleic Acids Res.* **2009**, *37*, e45–e45.
- (29) Pfaffl, M. W.; Horgan, G. W.; Dempfle, L. Relative Expression Software Tool (REST©) for Group-wise Comparison and Statistical Analysis of Relative Expression Results in Real-time PCR. *Nucleic Acids Res.* **2002**, *30*, 36e–36.
- (30) Lu, P. P.; Xu, Z. L.; Yang, H.; Wei, Y. M. Processing-structure Property Correlations of Polyethersulfone/Perfluorosulfonic Acid-nanofibers Fabricated via Electrospinning from Polymer-nanoparticle Suspensions. *ACS Appl. Mater. Interfaces* **2012**, *4*, 1716–1723.
- (31) Şimşek, E. N.; Akdag, A.; Çulfaz-Emecen, P. Z. Modification of Poly (Ether Sulfone) for Antimicrobial Ultrafiltration Membranes. *Polymer* **2016**, *106*, 91–99.
- (32) Belfer, R. F.; Purinson, Y.; Kedem, O. Surface Characterization by FTIR-ATR Spectroscopy of Polyethersulfone Membranes-unmodified, Modified and Protein Fouled. *J. Membr. Sci.* **2000**, *172*, 113–124.
- (33) Abdul Mannan, H.; Mukhtar, H.; Shima Shaharun, M.; Roslee Othman, M.; Murugesan, T. Polysulfone/poly (Ether Sulfone) Blended Membranes for CO₂ Separation. *J. Appl. Polym. Sci.* **2016**, *133*, 42946.
- (34) Zhang, L.; Wan, M. Synthesis and Characterization of Self-assembled Polyaniline Nanotubes Doped with D-10-Camphorsulfonic Acid. *Nanotechnology* **2002**, *13*, 750–755.
- (35) Low, K.; Chartuprayoon, N.; Echeverria, C.; Li, C.; Bosze, W.; Myung, N. V.; Nam, J. Polyaniline/poly (ε-caprolactone) Composite Electrospun Nanofiber-based Gas Sensors: Optimization of Sensing Properties by Dopants and Doping Concentration. *Nanotechnology* **2014**, *25*, 115501.
- (36) Pawar, S.; Patil, S.; Chougule, M.; Raut, B.; Sen, S.; Patil, V. Camphor Sulfonic Acid Doped Polyaniline-Titanium Dioxide Nano-

composite: Synthesis, Structural, Morphological, and Electrical Properties. *Int. J. Polym. Mater.* **2011**, *60*, 979–987.

(37) Li, C.; Chartuprayoon, N.; Bosze, W.; Low, K.; Lee, K. H.; Nam, J.; Myung, N. V. Electrospun Polyaniline/poly (Ethylene Oxide) Composite Nanofibers Based Gas Sensor. *Electroanalysis* **2014**, *26*, 711–722.

(38) Tapia, A.; Del Rosario, E.; Basilia, B.; Sarmago, R. FTIR and XPS Analyses of Thermally Aged Polyaniline Emeraldine Films: Relationship to Morphological and Electrical Properties after Doping. *J. Nucl. Relat. Technol.* **2009**, *6*, 27–40.

(39) Abbott, F.; Hong, Y.; Blier, P. Activation of 5-HT 2A Receptors Potentiates Pain Produced by Inflammatory Mediators. *Neuropharmacology* **1996**, *35*, 99–110.

(40) Shukla, R.; Singh, S. K.; Tripathi, A. Structural and Optical Study of Chemically Synthesized Polyaniline. *S-JPSET* **2015**, *7*, 33–35.

(41) Fung, Y.-C. *Biomechanics: Mechanical Properties of Living Tissues*; Springer Science & Business Media, 2013.

(42) Courtney, T.; Sacks, M. S.; Stankus, J.; Guan, J.; Wagner, W. R. Design and Analysis of Tissue Engineering Scaffolds that Mimic Soft Tissue Mechanical Anisotropy. *Biomaterials* **2006**, *27*, 3631–3638.

(43) Serena, E.; Figallo, E.; Tandon, N.; Cannizzaro, C.; Gerecht, S.; Elvassore, N.; Vunjak-Novakovic, G. Electrical Stimulation of Human Embryonic Stem Cells: Cardiac Differentiation and the Generation of Reactive Oxygen Species. *Exp. Cell Res.* **2009**, *315*, 3611–3619.

(44) Burkhard, S. B. *Origin and Function of the Cardiac Pacemaker*, Master's Thesis, Utrecht University, The Netherlands, 2011.

(45) Chi, N. C.; Bussen, M.; Brand-Arzamendi, K.; Ding, C.; Olgiv, J. E.; Shaw, R. M.; Martin, G. R.; Stainier, D. Y. Cardiac Conduction is Required to Preserve Cardiac Chamber Morphology. *Proc. Natl. Acad. Sci. U. S. A.* **2010**, *107*, 14662–14667.

(46) Trollinger, D. R.; Rivkah Isseroff, R.; Nuccitelli, R. Calcium Channel Blockers Inhibit Galvanotaxis in Human Keratinocytes. *J. Cell. Physiol.* **2002**, *193*, 1–9.

(47) Zhao, M.; Pu, J.; Forrester, J. V.; McCaig, C. D. Membrane Lipids, EGF Receptors, and Intracellular Signals Colocalize and are Polarized in Epithelial Cells Moving Directionally in a Physiological Electric Field. *FASEB J.* **2002**, *16*, 857–859.

(48) Lin, J.; Lindsey, M. L.; Zhu, B.; Agrawal, C.; Bailey, S. R. Effects of Surface-modified Scaffolds on the Growth and Differentiation of Mouse Adipose-derived Stromal Cells. *J. Tissue Eng. Regener. Med.* **2007**, *1*, 211–217.

(49) Yan, X.; Chen, J.; Yang, J.; Xue, Q.; Miele, P. Fabrication of Free-standing, Electrochemically Active, and Biocompatible Graphene Oxide– Polyaniline and Graphene– Polyaniline Hybrid Papers. *ACS Appl. Mater. Interfaces* **2010**, *2*, 2521–2529.

(50) Porter, G. A.; Makuck, R. F.; Rivkees, S. A. Intracellular Calcium Plays an Essential Role in Cardiac Development. *Dev. Dyn.* **2003**, *227*, 280–290.

(51) Suzuki, Y.; Ikeda, T.; Shi, S.; Kitta, K.; Kobayashi, Y.; Morad, M.; Jones, L.; Blumberg, J. Regulation of GATA-4 and AP-1 in Transgenic Mice Overexpressing Cardiac Calsequestrin. *Cell Calcium* **1999**, *25*, 401–407.

(52) Xia, Y.; McMillin, J. B.; Lewis, A.; Moore, M.; Zhu, W. G.; Williams, R. S.; Kellems, R. E. Electrical Stimulation of Neonatal Cardiac Myocytes Activates the NFAT3 and GATA4 Pathways and Up-regulates the Adenylosuccinate Synthetase 1 Gene. *J. Biol. Chem.* **2000**, *275*, 1855–1863.